IEEE Access
Multidisciplinary | Rapid Review | Open Access Journal

Received 23 November 2023, accepted 12 December 2023, date of publication 18 December 2023,
date of current version 28 December 2023.

Digital Object Identifier 10.1109/ACCESS.2023.3344041

TOPICAL REVIEW

A Review of Inductive Power Transfer: Emphasis on Performance Parameters, Compensation Topologies and Coil Design Aspects

MASOOD REHMAN[1], SOHRAB MIRSAEIDI[2], (Senior Member, IEEE), NURSYARIZAL MOHD NOR[3], MOHSIN ALI KOONDHAR[1], MUHAMMAD AMMIRUL ATIQI MOHD ZAINURI[4], ZUHAIR MUHAMMED ALAAS[5], (Member, IEEE), ELSAYED TAG-ELDIN[6], NIVIN A. GHAMRY[7], AND M. M. R. AHMED[8], (Member, IEEE)

[1]Department of Electrical Engineering, Quaid-e-Awam University of Engineering, Sciences and Technology, Nawabshah, Sindh 67480, Pakistan
[2]School of Electrical Engineering, Beijing Jiaotong University, Beijing 100044, China
[3]Department of Electrical and Electronics Engineering, Universiti Teknologi PETRONAS, Seri Iskandar, Perak 32610, Malaysia
[4]Department of Electrical, Electronic and Systems Engineering, Faculty of Engineering and Built Environment, Universiti Kebanngsaan Malaysia (UKM), Bangi, Selangor 43600, Malaysia
[5]School of Engineering, Jazan University, Jazan 45142, Saudi Arabia
[6]Faculty of Engineering and Technology, Future University in Egypt, New Cairo 11835, Egypt
[7]Faculty of Computers and Artificial Intelligence, Cairo University, Giza 12613, Egypt
[8]Faculty of Technology and Education, Helwan University, Helwan, Cairo 11795, Egypt

Corresponding author: Sohrab Mirsaeidi (msohrab@bjtu.edu.cn)

This work was supported in part by the Beijing Natural Science Foundation under Grant IS23051, in part by the National Natural Science Foundation of China under Grant 52150410399, and in part by the Fundamental Research Funds for the Central Universities under Grant 2019RC051.

ABSTRACT Wireless Power Transfer (WPT) using inductive and magnetic resonance coupling developing at enormous pace due to its diversity of applications, such as electric vehicles (EV), biomedical implants, consumer electronics, robotics and so on. This review presents historical background together with applications of low power and high power WPT systems. The review emphasizes on two main design facets of WPT system including compensation networks and coil structure. All up-to-date compensation topologies are comprised in the review along with latest coil designs. Load-independent operation using compensation topologies is also reviewed. The review provides all available methods to analyze the circuit structure of WPT system theoretically and it also outlines the software used for circuit simulations as well as coil design. This paper is diverse from existing reviews in a pattern that it presents not only complete critical intuition on the vital design features, recent advancements, contemporary problems and challenges of low power and high power WPT systems but also provides the available theoretical methods as well as software to analyze the WPT system in wholesome. This paper will enrich the knowledge of the researchers to investigate the WPT systems using existing techniques and to solve the present-day design glitches of WPT systems.

INDEX TERMS Wireless power transfer (WPT), inductive coupling, magnetic resonance coupling, coil design, compensation topologies, load-independent operation.

I. INTRODUCTION

Wireless Power Transfer (WPT) using inductive and resonant coupling works on the method of Power is transferred from the source to the load coil via electromagnetic induction (EI). WPT is applicable for short distance and medium-distance applications [1]. According to [2], the transmission distance between the source and the load coil, which is greater than the coils' diameter, is referred to as the WPT at medium distance. The short distance can be defined as the distance

The associate editor coordinating the review of this manuscript and approving it for publication was Diego Masotti.

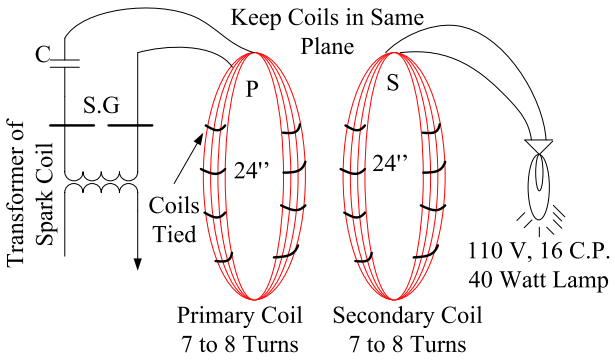

FIGURE 1. H. Winfield Sector's Tesla apparatus and experiments were published in Practical Electrics in November 1921.

between the coils is less than the diameter of the coils. WPT systems are complex in nature; therefore, various facets essential to consider formerly designing such systems. WPT was initially demonstrated at the end of the 19th century by Nikola Tesla [3]. Although tesla demonstrated the feasibility of a WPT system at the laboratory level, his wardenclyffe project was not successful. A resonant transformer often is known as an archaic. Tesla coil construction is depicted in Figure 1.

Where, the capacitor is receiving current from the high voltage transformer via the spark gap (S.G). At first, the spark gap is open-circuited, and current flows to the capacitor, charging it completely. When a capacitor's voltage rises too high, the spark gap breaks down and starts to function as a conductor. As a result, a shunt resonant circuit is created, and the capacitor's energy is released into the primary coil as a damped high-frequency oscillation. Through the resonance, a voltage gain from the secondary is made possible when this high-frequency current is oscillating in the primary coil. The primary coil inductance and capacitor value can be used to determine the natural resonance frequency [4]. After tesla's experiment, there has been little research on WPT technology due to the unavailability of high frequency switching devices at that time. Thereafter, the research on WPT using radioactive microwaves was conducted after 1960 [5], [6], [7], [8], [9], [10]. The radioactive technology uses far-field electromagnetic waves and has low transmission efficiency due to its unidirectional radiation pattern. It utilizes industrial, scientific, and medical (ISM) band (850 MHz – 2.4 GHz) [10]. Using RF and microwaves, power can be transferred over long distances using high-gain receiver antennas, but it requires sophisticated tracking and alignment mechanism and clear line-of-sight (LOS) in an unstructured and vigorous environment [5], [6]. William C. Brown proposed a WPT system based on microwave beams in 1966 [7]. To transform solar energy into electrical energy and then transmit it to the ground using microwave technology, Peter Glaser introduced the notion of building solar power stations in space in 1968 [11]. The near field inductively coupled wireless power transmission (ICWPT) was developed in the early twenty-first century. A method was made commercially available [12], [13], [14], [15], [16] for wirelessly charging low power devices such as toothbrushes and other portable electrical devices.

After that, the ICWPT was extensively researched how to handle high power applications up to a few kilowatts, such as charging electric automobiles for short distance applications with a grid to load efficiency of above 90% [17]. Figure 2 provides the historical development of WPT technology. Moreover, the resonant coupled wireless power transfer (RCWPT) method was suggested in 2007 by the researcher's team of Massachusetts Institute of Technology (MIT) as shown in Figure 3. At a 2m air gap, they could light a 60W bulb with an efficiency of 40% to 60% [18], [19]. In RCWPT system, the resonance can be achieved by self-resonance of the coils. However, in most cases the self-resonance frequency of the coils is much higher than the desired frequency; therefore the lumped capacitors can be added to achieve the desired resonance frequency.

After that, the circuit theory was explained in [20] for four coil structure using RCWPT technique. RCWPT is the modified form of ICWPT system, which utilizes high frequency than the ICWPT system and uses parasitic capacitance and self-inductances of the coil to achieve the resonating condition. It is difficult to create high-frequency high-power supply due to significant losses of high-power high frequency converters. Therefore, the ICWPT technique is widely used for high-power as well for low power applications. Recently, wireless charging pads are commercially available in the market for battery charging of cell phones, laptops, and computers. The EV battery charging is also progressing rapidly and charging spots in parking slots are being built in the developed countries [17]. ICWPT has also experimented for biomedical implants, such as capsule endoscopy, ventricular assist devices (VADs), battery charging of cardiac pacemaker and defibrillator [21], [22], [23], [24]. Wireless Power Transmission Market Size was priced at USD 7.8 billion in 2022. The wireless power transmission market industry is projected to grow from USD 9.3 Billion in 2023 to USD 28.6 billion by 2030, exhibiting a compound annual growth rate (CAGR) of 20.40% during the forecast period (2023-2030) [25].

The taxonomy of the WPT system for EV charging using various methods is depicted in Figure 2. The three main

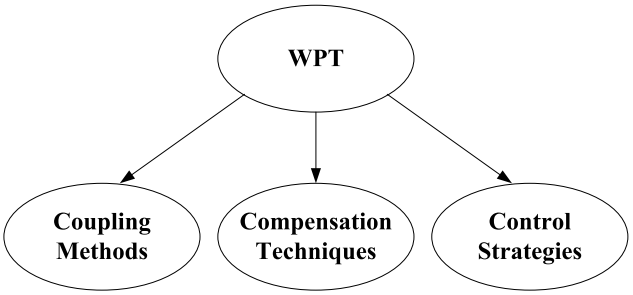

FIGURE 2. WPT taxonomy in different literatures [26].

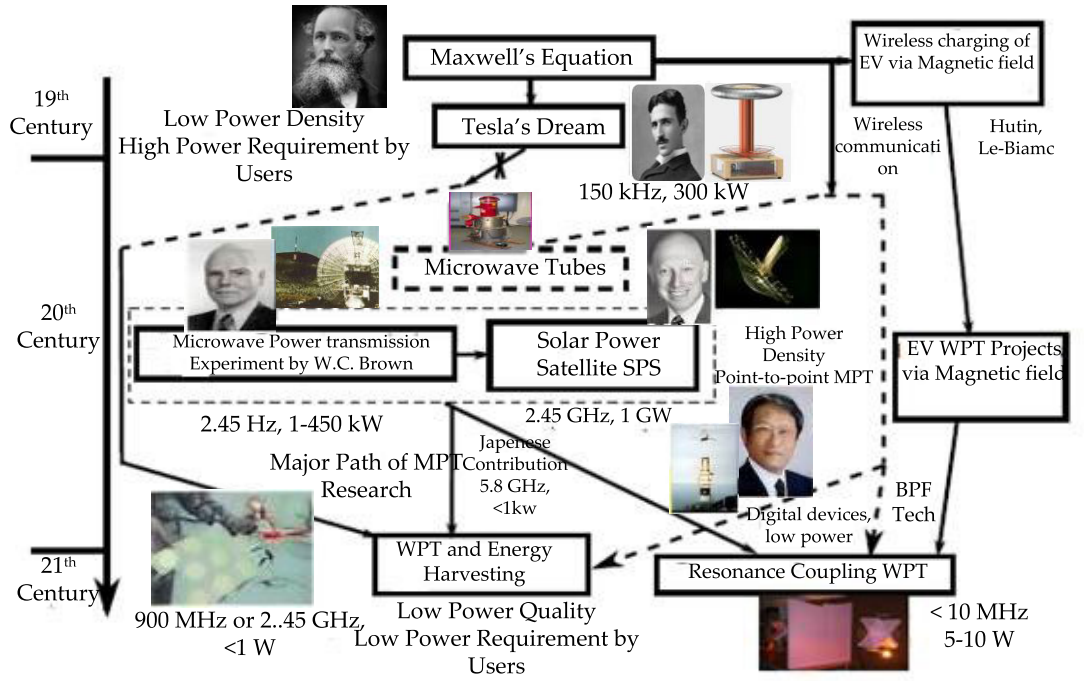

FIGURE 3. History of WPT technology.

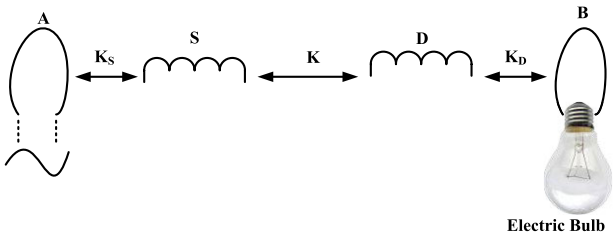

FIGURE 4. Schematic diagram of the experimental setup by MIT [18].

areas of WPT research were coupling topology, compensation strategies, and control methods [26].

The main factors which contribute towards the growth of usage of ICWPT devices are convenience and need for effective charging. However, non-standardized ICWPT charging systems lead to poor user experience and high cost, thus restricting the market growth [27]. Figure 4 depict the worldwide share of WPT market growth in recent years along with future prediction.

In addition to applications involving the transfer of electricity, these two sides can execute data communication, which could be of utmost significance. A thorough analysis of the transfer function of the power and data transmitting channels is done for the single link dual carrier (SLDC) approach. A design example for a Series-Series (SS) compensated system is shown for wireless charging applications for electric vehicles [28]. Along with power transmission, a wireless battery charging technique allows for the simultaneous transmission of information about the battery's state, the vehicle's ID number, and emergency messages between the grid and the vehicle. The secondary (vehicle) side operational state can be continuously monitored by the control system, and charging current can be changed in accordance with battery health [29].

The design of WPT can be described in four main facets; compensation topology, coil structure, control mechanism and power electronics, first two main facets are covered in this review. The behavior of efficiency can be easily understood by researcher in this review and load independent operation of different topology compensation. Numerous problems linked with the WPT technology, such as the quality factors of the coupled coils for receiving maximum efficiency are also discussed. The effects of coil misalignment on the efficiency and power transfer capability of the system are also comprised.

This paper is novel in way that it covers almost all the design aspects of a WPT system, such as, the compensation topologies, coil structures, control mechanism, power electronic devices, and human exposure. Moreover, it also provides the necessary tools available for conducting research in the domain of WPT technologies. Such as, all the available mathematical methods for WPT circuit analysis are provided in the Table 2, and the tools for simulation of WPT circuit are presented in Table 3.

Apart from that computer software tool for designing the coil structure and their analysis are given in Table 4. Also the tools available for co-simulation of coil structure as well as circuit design together are also provided. For example, Ansys Maxwell and Ansys Simplorer can be used together for

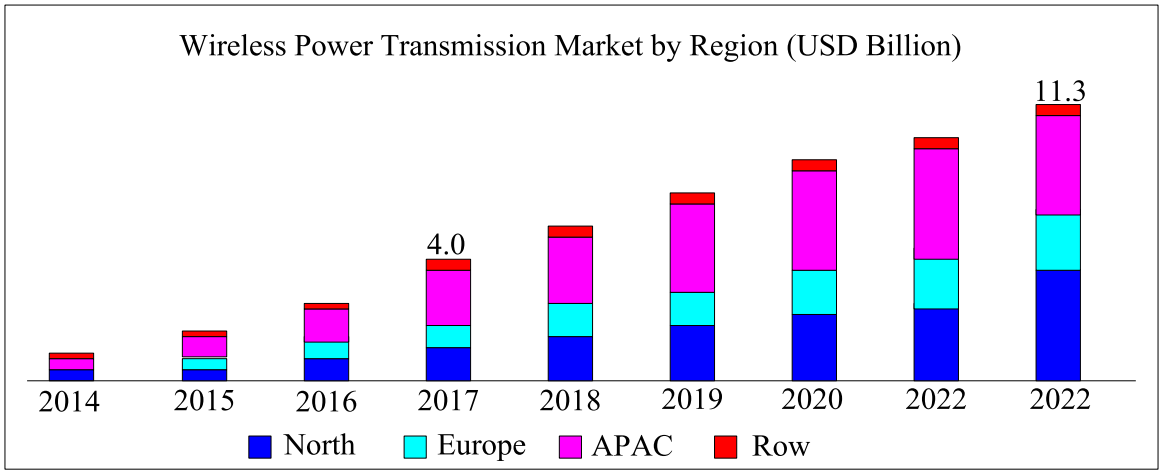

FIGURE 5. WPT market worldwide markets by region [2].

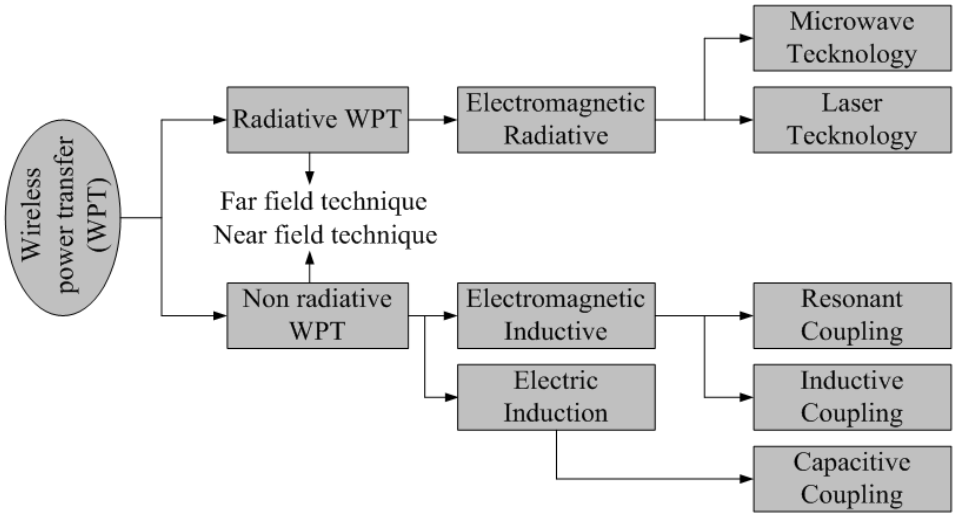

FIGURE 6. Different techniques of wireless power transfer [30].

combined simulation of coil structure and circuit at one platform, which is mentioned in Table 3. In that way, this review provides the broad and complete information for performing the research in WPT domain. Additionally, references from inductive coupled wireless power transfer and resonant coupled wireless power transfer are utilized to make this review more comprehensive.

II. DIFFERENT TECHNIQUES OF WIRELESS POWER TRANSFER

Different types of techniques have been utilized for WPT technology as illustrated in Figure 5, and different techniques of wireless power transfer are depicted in Figure 6.

Radioactive power is the ability to move energy over a distance that is typically several times greater than the transmitting antenna's dimensions, such as through air or a vacuum, in the form of an electromagnetic wave [2]. Radioactive WPT uses frequencies between 100 kHz to tens of MHz for industrial, scientific, medical, and defense applications [31], [32] and it offers low efficiency due to its unidirectional behavior [33]. Additionally, the radioactive power transfer method is not frequently used in civilian applications because its radiations might be harmful to human health. Recent developments in non-radioactive WPT research suggest that this technique may soon be more efficient and cost-effective for commercialization. Capacitive wireless power transfer (CWPT), inductively coupled wireless power transfer (ICWPT), and resonant coupled wireless power transfer (RCWPT) are three categories of non-radioactive WPT. Electric induction, which is the distribution of surface charges on the body or object, is the mechanism by which the capacitive WPT operates. In this technique, a high frequency voltage source excites a resonating transmitter to produce an alternating electrical field that couples with a resonating receiver and transmits power to the load. The efficiency of capacitive coupling, which may transfer

electricity over very small distances, is influenced by nearby bodies of water or other nearby objects [34]. The amount of power transfer is comparatively less than ICWPT and RCWPT. The capacitive coupling can be used for low power applications (1-50W) and relatively small distance (generally less than 1cm) [30].

During capacitive coupling, a small capacitance made by the electrodes gives a very high voltage between the electrodes, subjected to air breakdown. Capacitive coupling can be used for power transfer through a metal barrier [35]. Furthermore, the external magnetic field does not affect the capacitive coupling. Capacitive power transfer used in synchronous machines [36], low power contactless charging (5W) [37], and medical devices power supply (30W) [13]. Inductive coupling is a widely used technique; it works on the principle of electromagnetic induction like a transformer but uses high frequency (20 kHz to 1 MHz) than the transformer [33]. In a transformer, the electromagnetic field is naturally limited to a core of high permeability; however, ICWPT is different in a way that the region between the coils is air [38]. A high-frequency current is supplied to the transmitter (Tx) coil, which creates a magnetic field, and a voltage is induced through the magnetic flux in the receiver (Rx) coil. The leakage flux is generated because of air gap between Tx and Rx; however, in conventional transformer the leakage flux is neglected due to the negligible air gap. Besides, in inductive coupling, the leakage flux needs to be compensated by the external lumped capacitors or inductors by using different circuit topologies. Usually, the size of coils is bigger than the distance between the coils in ICWPT and it can be used for low as well as high power applications [2].

ICWPT enables a system to have an energy efficiency of over 90%. The tiny intervals between a few millimeters and tens of centimeters are appropriate for it. However, for the charging path to attain greater efficiency, exact alignment is necessary. The examples of ICWPT technology include the laptop and cell phones charging pads, chargers for electric toothbrushes and electrical vehicle charging, etc. RCWPT can be also called as the WPT using magnetic resonance coupling (MRC). RCWPT is suitable for medium distance transmission [39]. The medium distance means the distance between the coils is bigger than the dimension of the coils [2]. RCWPT technique is the modified form of ICWPT technique and it uses a higher frequency (generally between 5MHz and 20 MHz) than ICWPT. The magnetic resonance coupling is different from inductive coupling in a way that, the coupling between the transmitter (Tx) and the receiver (Rx) is achieved by both the magnetic field and the electric displacement field (electric flux density or free charge surface density). This is due to the high operating frequency (5 MHz – 20 MHz). The transmission is thus possible even in case of misalignment between Tx and Rx, but efficiency can be compromised. The main disadvantage of magnetic resonance coupling is that the maximum allowable field value is not yet known to ensure the safety of the users. Another drawback is that in the case of high-power applications, the power electronic devices using MHz frequency are difficult to implement due to the losses and high cost. ICWPT uses external lumped compensation capacitors for achieving resonance conditions, but in RCWPT self-resonance coils are preferred and their self-inductance and parasitic capacitances are used for achieving resonance condition. In case, the self-inductances and parasitic capacitances of coils are insufficient to create resonance at the required frequency, a lumped capacitor is required [2]. The literature's experimental findings and prior study lead us to the conclusion that RCWPT technology offers a number of advantages than ICWPT due to its higher transmission distance; however, it is appropriate for low power applications, because it uses high frequency (few MHz to several MHz) than ICWPT to achieve high-quality factor of coils [40], [41]. It is quite difficult to create high power and high-frequency supply due to many losses in power electronic devices. Therefore, for high power applications, the ICWPT technique is preferred.

Furthermore, the research reported in [42] presents a comparative analysis between RCWPT system and ICWPT system. It was demonstrated that the efficiency of RCWPT is greater than the ICWPT model due to its high frequency. However high-frequency supply is difficult to create in case of high-power applications. Moreover, in [20], a ''magic regime'' was discovered in the resonant coupling mode. A magic regime was defined as the regime where efficiency was constant over a certain distance. Additionally, it was reported in [43] that RCWPT and ICWPT will unite together in the future despite their present dissimilarities because both technologies are working in electromagnetic induction, the improved efficiency across long distances in RCWPT system is only due to high operating frequencies and high-quality parameters. The ICWPT and RCWPT have been used for multiple applications, such as the charging of electric vehicles, unmanned aerial vehicles (UAVs), biomedical implants and consumer electronic devices. WPT using inductive and resonant coupling possess certain advantages because of its high efficiency and reliability as compared to other methods. As mentioned earlier, there is a small difference between ICWPT and RCWPT techniques. ICWPT is more suitable for high power applications, while RCWPT can be a good choice for low power applications.

This review covers the ICWPT as well RCWPT techniques. However, more focus is kept on ICWPT technique. Although significant work has been done to improve both the techniques; however, many design challenges exist, such as efficiency decreases drastically with increasing distance, so it has limited transfer distance. Usually, a tradeoff between efficiency and transmission distance is taken into consideration. Higher efficiency is achievable at very short distances. High power can be transferred at long distances but efficiency becomes low. Furthermore, the quality factors of the coils play a vital part in the design of the WPT system. The quality factor of the coil depends upon the design of the coil and its

parasitic capacitances and intrinsic resistance value. While the loaded quality factor is also important factor in WPT system, it depends upon the compensation topologies and load resistance. Coil's quality factor increases with higher frequency, but to increase the frequency beyond a certain range is not feasible due to losses in power electronic devices. In case of a very high frequency, high-power inverters are difficult to implement due to their huge losses.

From the comprehensive literature survey, it can be extracted that there are four main design aspects of ICWPT system. First one is power electronics involved, second one is the design of charging coils / pads, and the third is the design of compensation network to create the resonance condition in order to transfer power at large air gaps with good efficiency. The fourth one is the implementation of proper control mechanism. This review will cover all the design aspects and their implications on the overall design of ICWPT system.

A. DRONES

The proposed frustum-shaped wireless charging port for UAVs and drones is depicted in Figure 7 via an image. The port has a truncated four-sided pyramid as its frustum shape, and it is manufactured of FRP. Even if large-sized UAVs hit the port on landing, the frustum-shaped port won't be broken because FRP is so strong. Since the frustum-shaped port is seamless, it is simple to guarantee its water proofness. Plastic does not impact the magnetic performance of transmits and receives coils. These FRP properties make them a good fit for wireless charging ports that use inductive power transfer. To conduct a preliminary assessment of inductive power transfer, the target drone has a receiving coil placed in its relatively thick vinyl chloride tube frame [44].

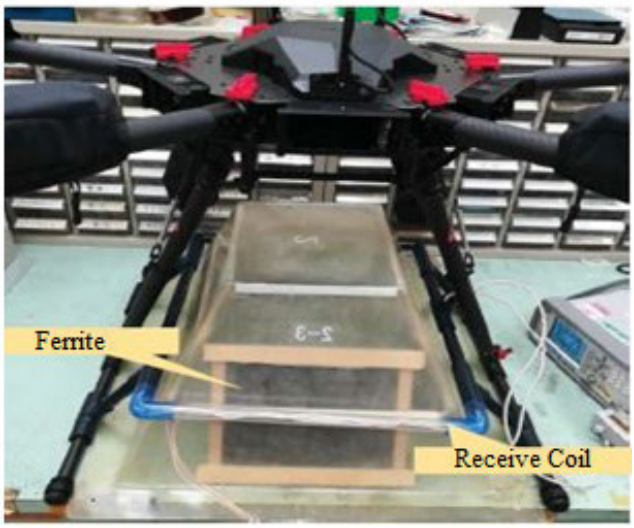

FIGURE 7. Wireless UAV/Drone charging FRP frustum port [44].

B. AUTOMATIC GUIDED VEHICLES (AGV)

Possibilities for WPT in transportation, such as vehicle electrification, EV, and AGVs are growing [45], [46]. Several studies have been devoted to examining the power transfer between vehicles and the grid, with a focus on both grid-to-vehicle (G2V) and vehicle-to-grid (V2G) interactions. However, the operating performance may be impacted by induced harmonics or unanticipated disturbances brought on by mismatched parameters and different resonant topologies during WPT [47], [48], [49], [50]. A dual-receiver system is provided for the standard AGV forklift utilized in unmanned factories, as seen in Figure 8. Through rectifiers and compensation networks, these two receivers guarantee two independent output channels. Additionally, all coils have spiral designs to increase rotational misalignment tolerance [46].

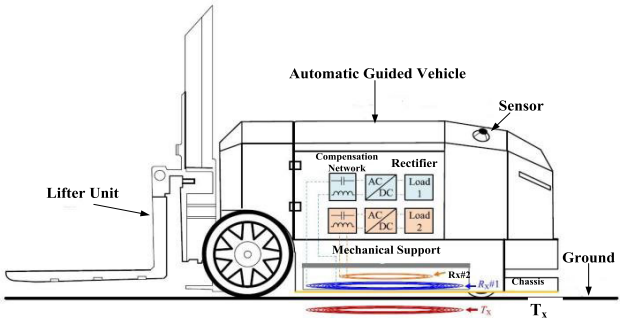

FIGURE 8. Typical AGV forklift schematic with the suggested two receiver setup [46].

C. ELECTRIC BIKES

One of the most potential EVs is the electric bicycle (EB), which has the advantages of convenience, low carbon emission, affordability, and user-friendliness [17]. However, the traditional charging method requires power lines to charge the battery, which in some severe situations may cause electrical leakage [51], [52]. Pioneers have investigated wireless power transfer (WPT) methods for EB charging systems to achieve this. For example, a double-coupled inductive system is suggested for multi pickup systems with the intention of wirelessly charging a fleet of EBs [53].

III. WORKING PRINCIPLE AND APPLICATIONS OF ICWPT SYSTEM

Figure 9 shows the fundamental structure of an ICWPT system. Initially DC supply is needed to convert it to high-frequency (HF) alternating current (AC) supply. Once HF-AC supply is created then compensation circuit is connected before the transmitter (Tx) coil. After that, the receiver (Rx) coil can be placed infront of Tx coil at some distance. Then the compensation circuit after the Rx coil is required. The role of compensation circuit is to resonate both Tx and Rx coil at the same frequency in order to achieve maximum efficiency. The Rx coil collects the induced voltage from the Tx coil and deliver it to the load. However, from the Rx side HF-AC is received, which cannot be used directly for load. Therefore, the rectifier circuit is employed to convert it to DC power first then it can be supplied to the load.

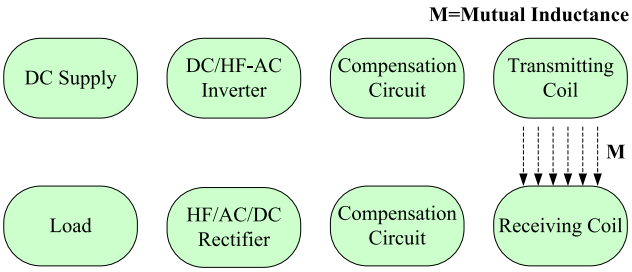

FIGURE 9. Fundamental diagram of ICWPT system.

A. LOW POWER AND HIGH-POWER ICWPT SYSTEM

The ICWPT system can be categorized into two parts according to the power level i.e. low power and high-power, as shown in Figure 10.

Both power levels got different challenges. Although some standards are available to commercialize low-power and high-power ICWPT devices to ensure interoperability between Tx and Rx. Still many standards need to be defined for further commercialization of ICWPT technology. The low power can be defined as the power from few mW to 100 W [54]. The high-power ICWPT systems can be described as the power above 1 kW. In low power systems, the small geometry of overall system is needed due to embedded design. Because low power application can be used for biomedical implants, which has size restriction especially from Rx side. Therefore, the efficiency is not the most significant factor in low power system. Besides, small size, higher tolerance in case of misalignment and low-cost are the most important factor for the designing of low power WPT systems. Moreover, in case of high-power system, the efficiency is an important, because large sized coils and high-power electronic devices are used for such system. Therefore, a small percentage drop in efficiency can cause the huge power losses of overall system. Therefore, power losses need to be minimized while designing such systems. In addition, the magnetic field emission is also a significant factor for low power as well as for high power applications to guarantee the safety of the user.

In recent years, ICWPT for EV charging is the most investigated field for high power applications. In general, two kinds of EV charging including stationary charging and dynamic charging are available. In stationary or static charging method, the transmitter and the receiver coils remain in stationary positions. In a dynamic charging method, the transmitter coils are fixed under the ground, while the receiver coils are embedded in a moving vehicle. In this way, the EV can be charged while vehicle is moving on the road. A systematic approach is required to design an ICWPT system for specific applications. Moreover, this section provides the further details of low power and high-power applications as follow.

B. APPLICATIONS OF LOW POWER ICWPT SYSTEM

Some important applications of low power ICWPT systems are provided below.

1) DESKTOP PERIPHERALS SUPPLY AND MOBILE PHONE CHARGER

In recent years, the ICWPT charging pads has become popular for consumer electronic devices, especially, for desktop peripherals, mobile phone charging pads, etc. The ICWPT for desktop computers and cell phones is broadly investigated. The required power for these devices lies between 1 to 20 W and the air gap between the coils is normally less than a cm. Wireless charging system for mobile phones was investigated in [43] using two circular coils with a 35 mm radius with frequency of 500 kHz. The system has transferred power of 4W up to 2mm distance between the coils. Moreover, in [55], a wireless charging system using desktop peripherals was designed. A battery manager was used for a controlled load battery cycle. To test the system, the cell phone devices were positioned on a ''charging pad'', as illustrated in Figure 11. The charging pad then detected the availability of one or more objects to starts the transfer of power wirelessly. It was noticed that the internal self-inductance decreased slightly with the frequency, but its value was negligible compared to the total inductance of the pad.

2) BIOMEDICAL IMPLANTS AND MEDICAL APPLICATIONS

ICWPT using inductive and resonant coupling got many applications for biomedical implants such as a cardiac pacemaker, cardiac defibrillator, spectral endoscopy, etc. In those conditions, it is difficult to send the power to charging plants using wires; therefore, the need for ICWPT is a quite useful technique in such situations. ICWPT for cardiac pacemaker using SS topology and sandwich structure was proposed in [23]. The sandwich structure of coils was made by two series-connected Tx coils and two series-connected Rx coils; however, both Tx coils kept outside the Rx coils to make it sandwich coils structure as shown in Figure 12 [56]. The proposed system provided the rated power output 4 W with a transmission efficiency of 88% and the transmitter current less than 1 A. The transmission distance was set as 200 mm. An LCC-C topology for ICWPT to charge the battery of pacemaker is utilized in [22], where C shows the series capacitor from the secondary side, which is illustrated in Figure 13 [58]. The research on capsule endoscopy is conducted in [24], a modified Helmholtz coil is proposed for high efficiency and better power stability. SP-mixed resonance scheme is utilized. ICWPT for endoscopy is shown in Figure 14.

3) RESONANT LOOPS

Domino and relay resonators have been used to improve the transfer distance of the ICWPT system. The ring resonators have also been employed [59], [60], [61]. Domino or relay resonators are defined as the intermediate coils between Tx and Rx to enhance the transmission distance. These coils can be self-resonant or resonating on the frequency adjusted by external lump capacitor. In [57], ICWPT using ring domino resonators were developed, as illustrated in Figure 15. The transmitter power was set as 15 W using a frequency of

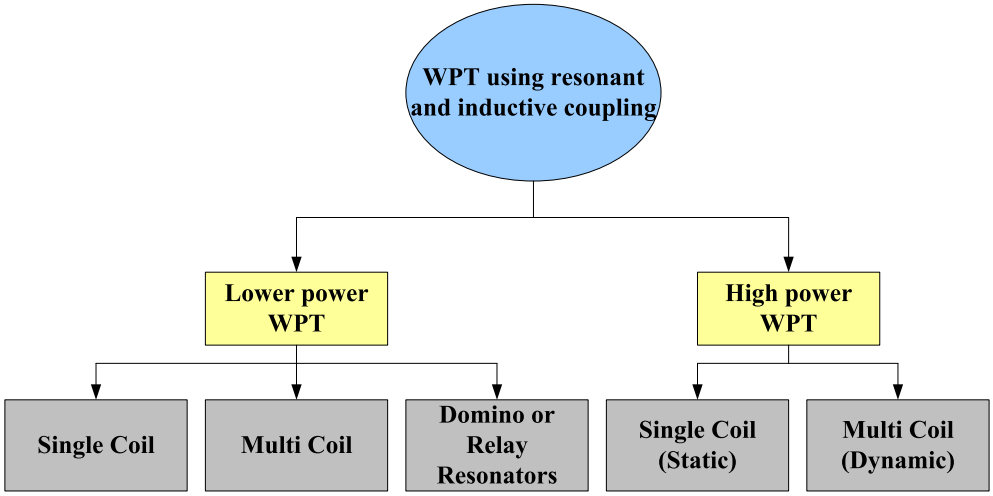

FIGURE 10. ICWPT Categorization according to power level.

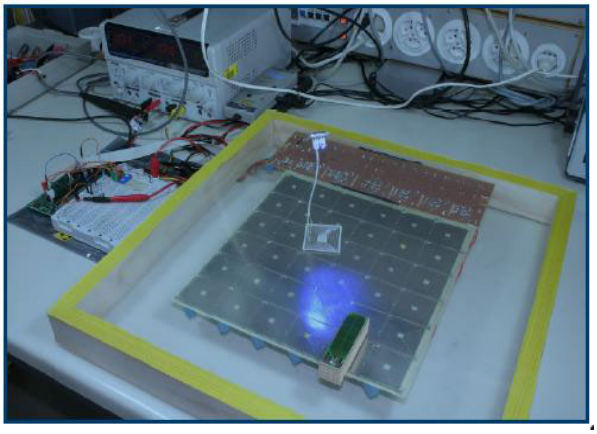

FIGURE 11. Desktop peripherals charger realized in [55].

500 kHz. Although this is a very sophisticated solution to enhance the air gap between the primary and secondary coils, no real application uses this concept in literature.

4) EXISTING STANDARDS FOR LOW POWER APPLICATIONS

To increase the interoperability between different types of devices made by different companies, it is necessary to have standardization for compatible charging of several devices. Figure 16 shows the concept of interoperability among different devices. Although many standards have been set for ICWPT, the probably most acknowledged standard for ICWPT is given by Wireless Power Consortium and is known as QI Standard for ICWPT for low power applications between 0 to 5 W for a distance up to 40 mm [31].

Moreover, three types of coils have been included, as illustrated in Figure 17 to improve coupling coefficient. The first one is named ''guided-positioning'' in which the device under charge is aligned to the transmitting coil. The second one is the ''free positioning'' having a dynamic coil. The primary coil moves below the receiving coil to keep the coupling factor in the desired position of the receiving coil. The third one is ''free positioning having coil matrix''. In this structure, the transmitter is made up of the coil arrays. In the multi-coils' setup, a method of detection of a load is done to supply the power to the only coils below the receiver. A canal-based information system to control the transmission of power by using reflected impedance values is superimposed to the power transfer canal. The standard also provides the definition of the communication protocol between the transmitting and receiving devices [62]. Furthermore, one more standard known as Rezence has been provided in 2012, by the company Alliance for ICWPT (A4WP). The power transfer up to 50 watts at a distance of 5 cm for an operating frequency of 6.78 MHz is included in this standard. This standard employs intelligent Bluetooth (BLE) to create a communication link between the transmitter and its device. The Power Matters Alliance (PMA) is another company, which is trying to standardize universally the diverse standards presented above together in one so that the ICWPT chargers can be easily used in public places as shown in Figure 18.

C. APPLICATIONS OF HIGH-POWER ICWPT SYSTEM

High-Power ICWPT can be referred to as usually the power transfer larger than one kW, and is applicable in case of EV charging and electric bicycles (EB) charging. In case of high-power applications, the losses need to be minimized in order to improve the efficiency. Low efficiency high power devices may produce extra thermal energy due to losses, which is not good for the environment and the safety of the charging devices. For safety concerns, the magnetic field emission should be minimized to limit the emission value according to ICNIRP commission standards according to frequency and application. The ICWPT chargers for ICWPT can be segregated into two parts, stationary charging and dynamic charging. In stationary charging, a car's battery

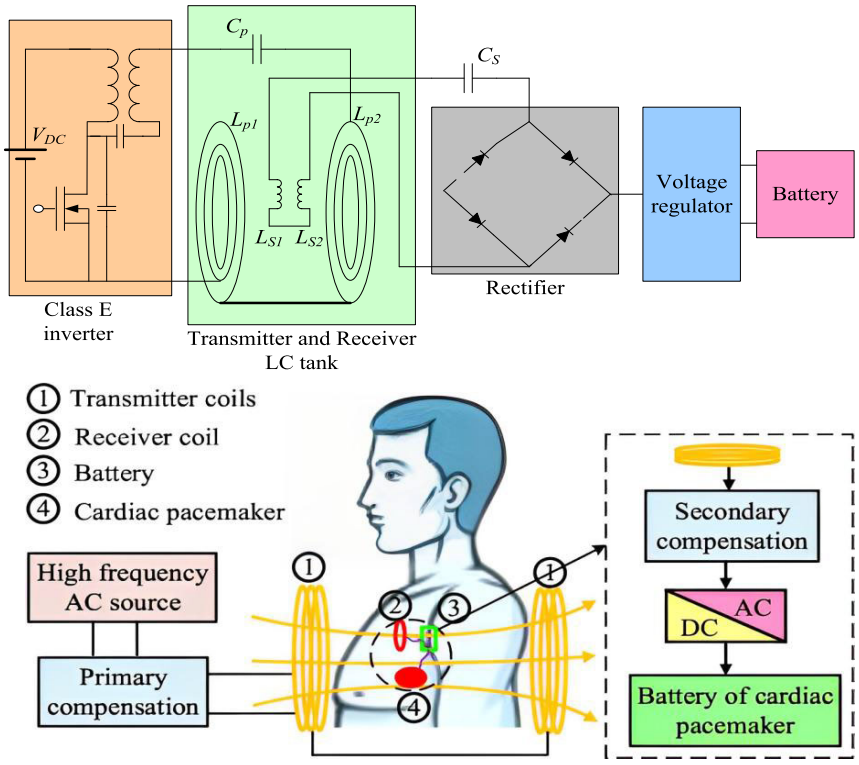

FIGURE 12. A sandwich ICWPT system for cardiac pacemaker [23], [56].

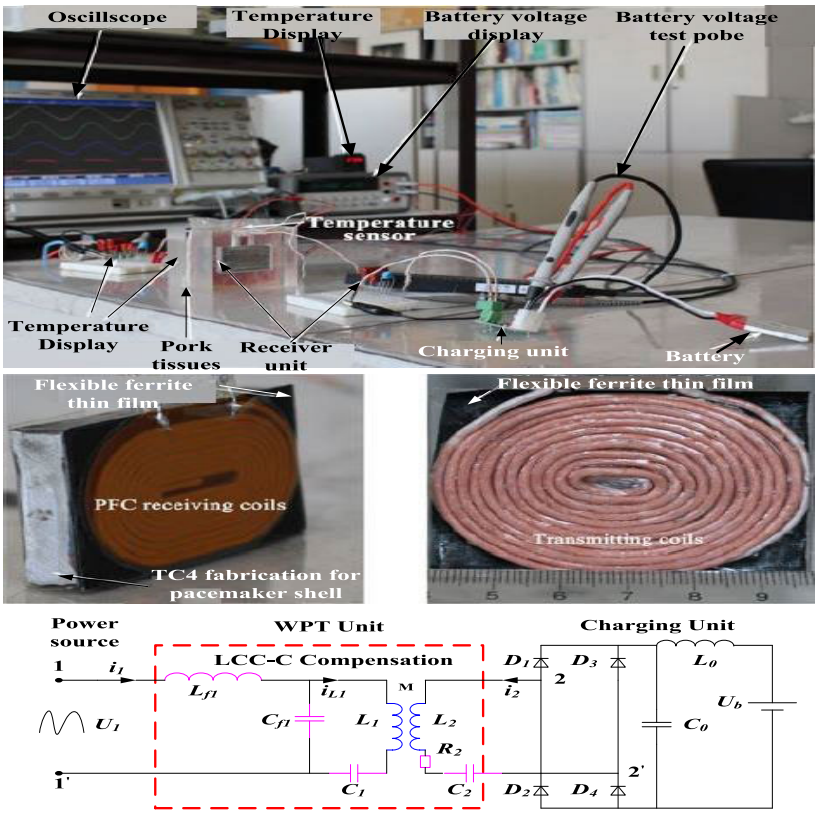

FIGURE 13. LCC-C topology for pacemaker charging proposed [22].

can be charged by parking the car on a specific slot, where the transmitter coil is kept on the ground or buried under the ground, while the receiver coil installed in car. The dynamic charging is defined as the battery charging of a

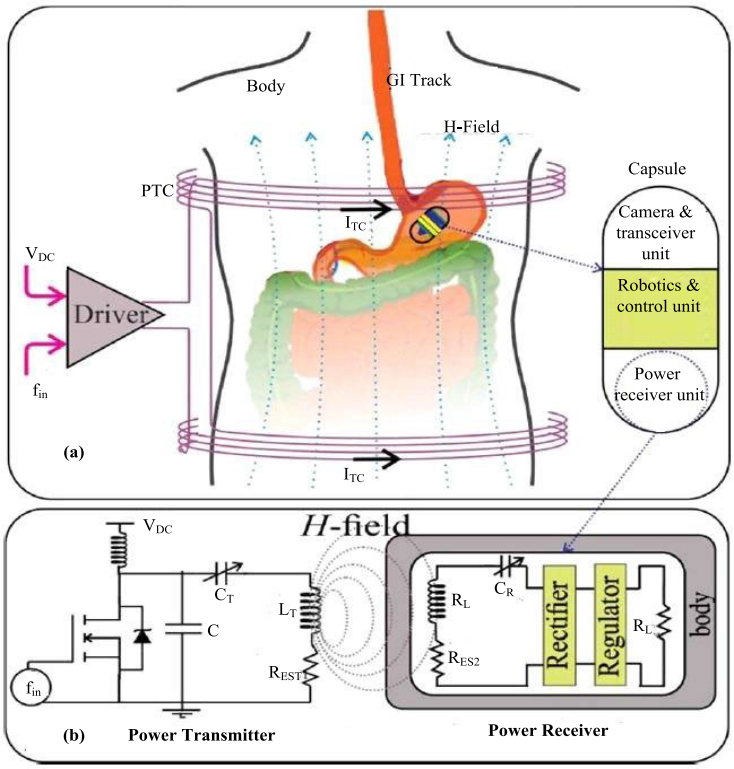

FIGURE 14. Schematic of an ICWPT system for endoscopy [24].

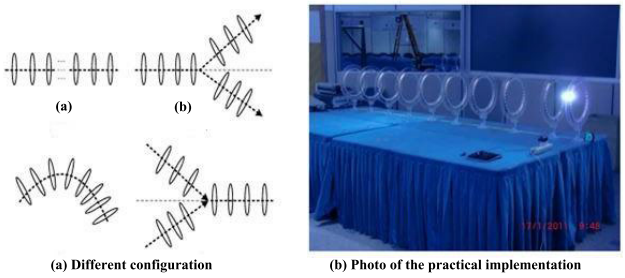

FIGURE 15. Resonant coils (resonators) [57].

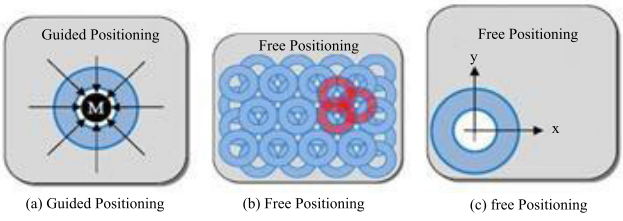

FIGURE 17. Configurations of Qi standards [31].

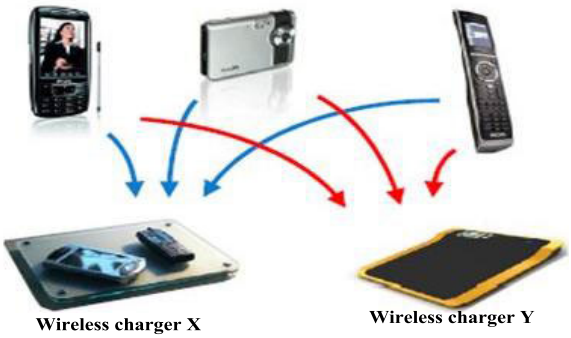

FIGURE 16. Interoperability concept [31].

FIGURE 18. ICWPT charging pads.

car in motion during driving on the roadway [63], [64]. In dynamic charging method, the size of the battery can be reduced; consequently overall EV weight can be reduced. However, dynamic charging suffers from low efficiency due to misalignment, and power fluctuation [40], [65], [66], [67]. Presently, stationary charging is the widely used technique due to its high efficiency and simple control mechanism as compared to dynamic charging. Further details regarding both the charging mechanisms are provided below.

(a)

(b)

FIGURE 19. Transformers for high power applications (a) [69] (b) [68].

1) STATIONARY CHARGING OF ELECTRIC VEHICLE AND ELECTRIC BICYCLES

The stationary or static vehicle charging can be defined as when a car is parked in a specific slot, where it can be charged. In recent decades many researchers are working on the improvement of ICWPT technology for charging the battery of electric vehicles (EVs). The transmitter side power is usually in the range of 1 kW to 200 kW using an operating frequency of around 20 kHz to 100 kHz. As the HF inverter and other electronic need for high power are more complex than for low power applications, coil arrays are generally avoided. For high power, ICWPT applications bulk iron parts are present near to the ICWPT system, such as the EV itself. When the proper shielding is not employed, then much power may be dissipated in the bulky iron parts. Therefore, shielding is mandatory for the design of a high power ICWPT system. The authors proposed a shielding made up of an aluminum sheet and a ferrite plate at both the primary and secondary side to reduce these power losses [68].

As depicted in Figure 19 (b), the primary side coil is larger than the secondary side to improve the misalignment tolerance. The exact dimensions of the coils are not given. In this system, the operating frequency was around 140 kHz.

In [70], a 3-kW ICWPT system for charging a battery was proposed using 100 kHz frequency; however, the transmission distance was very low around 5mm, having coupling factor (k) of 0.8. The research of Saragossa University developed a 5 kW ICWPT battery charger using 15 kHz frequency, as shown in Figure 19 (a) [69]. They achieved an efficiency of 94%. However, no shielding or ferrite material was employed. The proposed system has fewer losses because of only two coils used, as no other iron parts, such as a car or any other vehicle were placed in the vicinity of the two coils.

In [71], the authors proposed an ICWPT system using a special coil geometry to reduce the effect of misalignment. In this method, the coils were placed around the ferrite bars, as shown in Figure 20.

This system had a power capacity of 2 kW to supply to the EV. This type of configuration is usually not good for interoperability with other coils, because, in this proposed configuration, the secondary coil is sensitive to a tangential component only; however, most transmitting coils use the vertical component. To overcome this issue, a basic secondary pad using multiple coils called ''Quadrature Double D with quadrature coil'' as depicted in Figure 21 was proposed in [66] and [72].

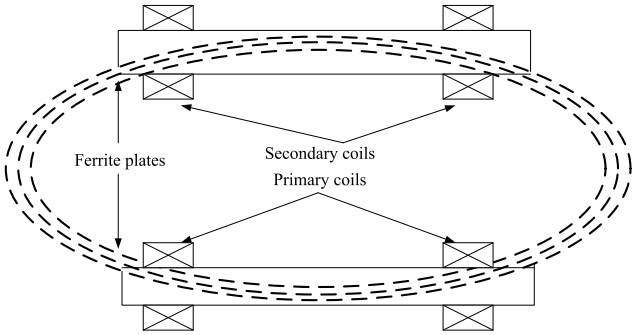

FIGURE 20. Geometry proposed to increase the misalignment tolerance [71].

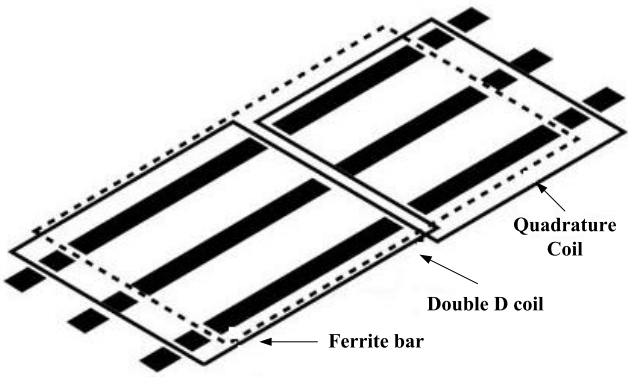

FIGURE 21. Double D with quadrature coil [66].

2) DYNAMIC ELECTRIC VEHICLE POWER SUPPLY AND BATTERY CHARGER

In the dynamic charging environment transmitter side is static while the receiver side is continuously moving, which is also called the ''pick-up'' side. The dynamic charging of EVs is also called Roadway Powered Electric Vehicles (RPEVs). Dynamic electric vehicle charging is more challenging than a static one because, it has more challenges such as, misalignment angle, which can significantly reduce the amount of power to be transferred to the receiver. Many researchers have given the ideas to cope with the issues of dynamic

charging and some solutions have been provided in the literature. A simple solution was presented in [73] by designing very long single coils from the primary side, as illustrated in Figure 22 (a). In this design, the moving secondary part remains always above the primary (transmitter) side coil to enhance the receiving capability of the receiver. Additionally, the secondary (receiver) coil was made of two coils combined in a way than one coil is sensitive to the tangential component of the other one to the normal component of the magnetic field. Another design was proposed in [74], to cope with the misalignment of the coils by designing more primary tracks as depicted in Figure 22 (b). The main problem of this configuration is the interaction between the primary coils, which may cause losses. Some special geometry are investigated to reduce this effect between the primary coils, as investigated in [75].

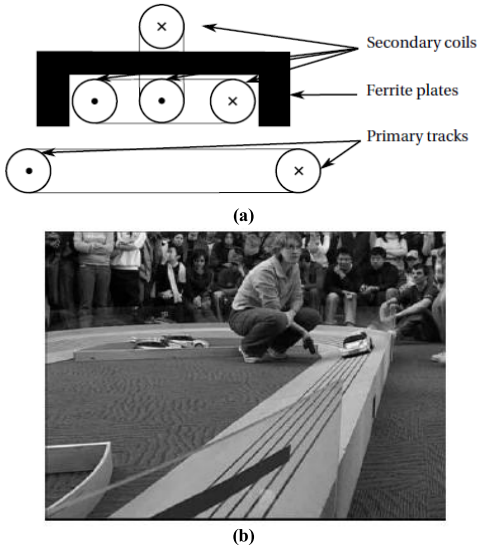

FIGURE 22. (a) A proposed solution of moving secondary part (b) Prototype [74].

Figure 23 (a) shows a primary coil track without interaction cancellation and Figure 23 (b) shows the track with interaction cancellation.

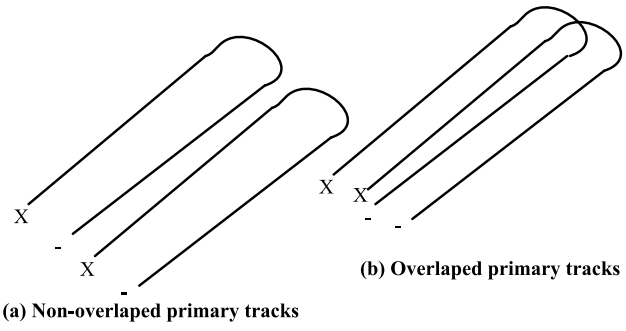

FIGURE 23. Description of the multi-track for pickup applications [68].

The drawback of such tracks structure is that they are huge and need to supply all the tracks, in that way the efficiency is reduced because of power dissipation in large tracks. In terms of safety, the magnetic field emission becomes too high where the pickup secondary coil is not available. This problem can be solved by dividing the roadway into smaller coils and power should be supplied only at the specific place where the vehicle is presented in real-time. Such structure by detecting the vehicle available and supply the power only to the corresponding primary coils has been realized in the "Laboratoire d'electromecanique et de machines electriques" at "Ecole Polytechnique Fédérale de Lausanne" for electric transportation vehicle called "Serpentine" [76].

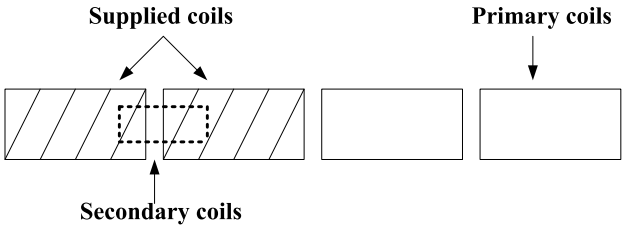

FIGURE 24. The solution implemented for the "Serpentine" project.

FIGURE 25. Serpentine systems of installation of track.

This implementation is illustrated in Figure 24, Figure 25 and Figure 26. Only the hashed coils were supplied by the power mains, so that the power losses and field emission can be reduced. However, this system did not include the magnetic shielding. Moreover, a cordless inductive power transfer for an electric bus was proposed in [77], [78], [79], and [80], as depicted in Figure 27. This system was called as OLEV (On-Line Electric Vehicle). The distance between the primary and the secondary parts was 25cm and the total power transmitted was 100 kW using 20 kHz operating frequency. Due to very high power, the frequency was kept low. Table 1 displays the ICWPT systems used for EV charging in various nations.

IV. TOOLS/ METHODS USED FOR CIRCUIT ANALYSIS OF WPT SYSTEM

There are several methods, which can be used to analyze the circuit design of WPT system, which are briefly explained in Table 2. These methods are useful for new researchers in the

TABLE 1. ICWPT system implemented for EV charging in different countries.

Ref	Name of Country	Power	Airgap between the Tx and Rx coils	Efficiency of the System
[88]	USA	20 kW	25 mm	--
[89]	New Zealand	30 kW	45 mm	--
[90]	USA	2 kW	75 mm	91% (coil to coil)
[91]	South Korea	100 kW	200 mm	75%
[92]	Japan	1.5 kW	70+_ 20 mm	95%
[93]	Switzerland	5 kW	52 mm	96.5%
[94]	Switzerland	50 kW	160 mm	95.8%

TABLE 2. WPT circuit analysis methods.

Ref.	Name of method	Procedure for simplification of circuit
[57, 95, 96]	Norton's theorem	It considers a single value of all the impedances, which are calculated by considering them parallel to a current source by created short circuit across two designated nodes
[57, 97, 98]	Thevenin's theorem	This theorem considers a single value of all the impedances, which can be calculated as series to a voltage source by creating open circuit across two selected nodes
[99-102]	Kirchhoff's voltage law (KVL)	KVL can be defined as the algebraic sum of all the voltages including voltage drop and source voltage around a closed path is equal to zero.
[103]	Kirchhoff's current law (KCL)	KCL can be defined as the sum of all currents into a node is equal to the sum of all currents out of that node.
[104, 105]	Superposition theorem	Superposition works on the principle of taking at a time one power source in the whole circuit to determine the voltage drop and current across each component/impedance. Then, the current and voltage drop across each impedance during all active power sources can be algebraically added.
[106-108]	Two-port network (ABCD) parameters	In 'ABCD' matrix, A and C letters can be calculated by open circuit test. While B and D is calculated by short circuit test. All letters provide the ratio of input voltage or input current to output voltage or output current. Power source and load is excluded in this analysis.
[109]	Two-port network impedance (Z) parameters	Impedance (Z) parameters are useful for calculating impedances of two port network by ratio of input or output voltage over input or output currents using short circuit and open circuit test. Power source and load is excluded in this analysis.
[42, 84, 106, 110]	Two-port network (S-parameter)	Scattering or S parameters are defined in terms of incident or reflected waves at ports. Each S parameter is the ratio of voltages of input and output ports in two situations, i.e. by terminating port 1 or by terminating port 2.
[107, 111-113]	Smith chart	It is based on graphical chart, can be used for impedance matching design and measuring the unloaded Q-factor. It is also useful for investigation of circuit behavior of high-frequency (HF) devices such as HF inverter and amplifier.
[102, 103, 114]	Fundamental harmonic analysis (FHA)	In this method, frequency analysis is performed by neglecting all the higher order harmonics. Only the fundamental component of square waveform or sinusoidal waveform is considered.
[18, 19]	Coupled mode theory	It analyzes the energy exchange between resonant coupled objects (within space) in time domain.

TABLE 3. Software used for circuit simulations.

Ref.	Software/Tool	Description
[84, 112, 113, 115]	Keysight's advanced design system (ADS)	Used for smith chart analysis, circuit simulations especially good for high frequencies in MHz, also can be used for low frequencies
[111, 116-118]	MATLAB/Simulink	Used for circuit simulations, MATLAB used for graphs, calculations using equations in MATLAB and optimization algorithm implementation.
[25, 59, 117]	PSpice simulation software	Used for circuit simulations
[96, 104, 119, 120]	LTspice	Used for circuit simulations
[121]	Ansys-Maxwell &/or Simplorer	Simplorer is used for circuit simulations. Ansys-Maxwell and Simplorer together can be used for combined simulation of coils structure along with lumped circuit model.

field of WPT technology. Moreover, different software/tools have been utilized in previous research to simulate the WPT circuit are presented in Table 3. Furthermore, the different methods used for design of coil structure are presented in Table 4.

V. COMPENSATION TOPOLOGIES OF ICWPT SYSTEM

The four basic compensations are SS, SP, PS, and PP, with the first S or P standing for series (S) or parallel (P) compensation from the primary side and the second S or P standing for series (S) or parallel (P) compensation from the secondary

TABLE 4. Software/tools and methods used for coil design.

Ref.	Software/Tool	Description
[117, 122, 123]	Ansys-Maxwell	Based on finite element method for calculation of magnetic field, self and mutual inductance between the coils
[124, 125]	COMSOL Multiphysics	Based on finite element method for calculation of magnetic field, self and mutual inductance between the coils
[100]	JMAG Designer	Based on finite element method for calculation of magnetic field, self and mutual inductance between the coils
[126]	Biot–Savart law	Magnetic field calculation of coil
[42]	Neumann's Formula	Magnetic field, self and mutual inductance calculation between coils

FIGURE 26. Serpentine systems showing the vehicle.

side, respectively. In [14] and [81], these fundamental topologies were explored. In [82] gave a comparison of two- and three-coil topologies and offered a straightforward method for determining the WPT circuit characteristics for charging electric vehicles. Three-coil structures were shown to be more effective and tolerable to misalignment between the transmitter (Tx) and receiver (Rx), respectively. In [20] offered a thorough analysis of the four-coil structure. Additionally, [83] proposed a circuit layout with series and parallel mixed compensation from the primary and secondary sides. Mixed compensation has been demonstrated to be capable of offering good efficiency even with non-symmetrical loads. At a distance of 10 cm, the efficiency was 85%, while at a distance of 20 cm, it was just 45%. Relative distance was a novel phrase that was defined as a distance in relation to the size of the coils. Not only does it specify how far apart Tx and Rx are, but also how long that distance is for example, the length of two coils. A Series/Capacitor Inductor Capacitor compensation topology, which has the advantage of constant output voltage with zero phase angle and zero voltage switching, was also proposed by [58].

The power transfer efficiency and output capacity of a WPT system are greatly reduced by the axial and angular misalignment between magnetically connected coils [84]. Coil misalignment causes the primary coil driver to function in an unturned state, which leads to less-than-ideal switching behavior and an increase in switching losses, according to [65]. To reduce the negative consequences of misalignment between the magnetically connected coils, it would be helpful to investigate the tuning mechanism. Additionally, [60] discusses WPT based on Domino-Resonator Systems with Non coaxial Axes and Circular Structures. In [59] used relay resonators to increase the transfer distance between the source and load coil. There are several challenges and issues in designing the complete ICWPT system, due to ramifications of the charging coil structure, compensation topology, power electronics involved and control mechanism. Before developing the ICWPT systems, other factors such as the size of the transmitter and reception coils, the operating voltage and current carrying capability, and the compensation topology must be taken into account. Series-series (SS), series-parallel (SP), parallel series (PS), and parallel-parallel (PP) are the four fundamental compensation topologies that have been extensive. The first S or P denotes the series or parallel compensation of the Tx coil, and the second S or P denotes the series or parallel compensation of the Rx coil [81], [85]. In [82], a comparison between two- and three-coil designs was published, and a more straightforward method of determining the ICWPT circuit characteristics for charging electric vehicles was offered. The three-coil construction was shown to be more effective and tolerable to misalignment between the transmitter (Tx) and receiver (Rx), respectively. All three coils employ a series compensation topology offered a thorough analysis of the four-coil structure [20]. A circuit layout that incorporates mixed series-parallel compensation from the primary and secondary sides was also proposed in [83] and [86].

Mixed compensation has been demonstrated to be capable of offering good efficiency even with non-symmetrical loads. For distances of 10 cm and 20 cm, the efficiency was 85% and 45%, respectively. Relative distance was a new phrase that was defined as a distance in relation to the size of the coils. It simply does not specify the distance between Tx and Rx but rather the length of the distance, such as the double of the coils. Additionally, a Series/CLC compensation scheme with zero phase angle and zero voltage switching was proposed in [58], which has the benefit of constant output voltage. The power transfer efficiency and output capacity of an ICWPT system are greatly reduced by the axial and angular misalignment between magnetically connected coils. The primary coil driver operates in an unturned condition as a result of coil misalignment, which results in less-than-ideal switching

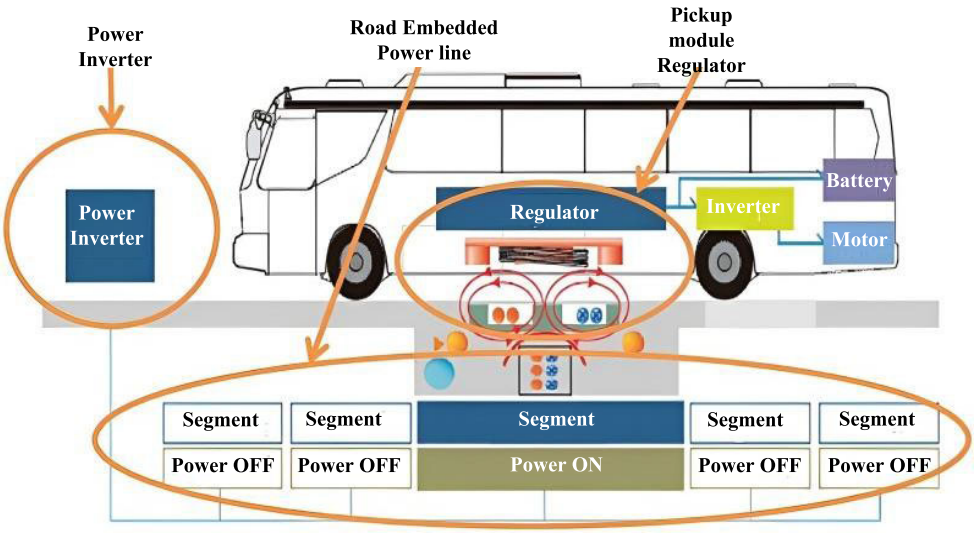

FIGURE 27. Layout of the dynamic EV charging system proposed [76].

operations and an increase in switching losses [65]. To reduce the negative consequences of misalignment between the magnetically connected coils, it would be helpful to investigate the tuning mechanism. Also covered in [50] is ICWPT based on Domino-Resonator Systems with Non-coaxial Axes and Circular Structures. In this study, relay resonators were used to increase the transmission distance between the source and load coils [59], [126].

To increase the effectiveness of the ICWPT system, numerous circuit topologies have been investigated. Unsymmetrical coils have not been used, however secondary series and parallel topology analysis for inductive power transmission is done in [16] along with a discussion of load-independent voltage transfer. In order to charge the batteries with constant current and constant voltage, hybrid topologies for ICWPT are researched [127]. In [92], modeling and Pareto optimization of ICWPT coils for electric vehicles were done using the two distinct topologies of SS and SP. In [112], a generic theory with a focus on SP-Combined topology was investigated, and efficiency equations were derived. In [128] and [129] gave an analysis of ICWPT utilizing SS and SP-Combined Topology. In [130] put forth and optimization method for raising ICWPT's effectiveness. A metamaterial-based finite element analysis of an ICWPT system was presented in [131]. In [132] describes the design and simulation of a multiple coil model for the ICWPT system. Inductive coupling and equations of resonant frequency were used to analyses wireless power transfer in [133].

From the literature review of compensation topologies, it can be extracted that the Rx side capacitors can improve the power transfer capability by compensating the leakage inductance of the receiver and mutual inductance [134]. While a capacitor from the Tx side can be useful for achieving the unity power factor by compensating the self-inductance of primary coil as well as the inductance of whole circuit. In [135] ICWPT using SP-mixed compensation was designed and its characteristics using varying loads were analyzed. Four combinations of capacitive IMNs were considered, i.e., SP in a transmitting side (Tx) and SP in a receiver (Rx) side (SP-SP), SP-PS, PS-SP, and PS-PS. The optimum capacitance values for each IMN were also derived. For verification, three cases based on the number of Rx coils were considered to verify the calculated results with simulations and measurements. It was found that a single Tx and a single Rx provides similar efficiency in all the four combinations. However, in multi-receiver ICWPT systems with the PS compensation from Rx sides were found to transfer more power towards Rx coil, but it was suitable for lower load impedances and was sensitive to load variation. On the other hand, using the SP compensation from Rx sides was less sensitive to load variation than the PS counterpart. In addition, an ICWPT system using the SP-SP combination was more reactive to the cross-coupling between Rx coils than the PS-PS compensation.

A. SS COMPENSATION NETWORK

SS compensation topology consists of series capacitor from Tx and Rx side as shown in Figure 28 (a). There are two ways to design the capacitor of SS topology, i.e. compensation with self-inductance of coils or compensation of the leakage inductance. When capacitor are designed to compensate according to the self-inductances of primary and secondary coils and tuned to a resonant frequency, then the output voltage of SS topology is sensitive to load variations [136], but maximum power transfer at certain coil current can be achieved [137]. If capacitor is designed to resonate with the leakage inductance, then a higher ratio between the active power to reactive power can be achieved [116]. A comparison of self-inductance tuning and leakage inductance tuning of SS topology was provided in [138] and [139]. To achieve

load-independent output voltage using SS compensation, the coils can be tuned to the frequency of load-independent voltage gain [138], [139]. However, the zero-phase angle (ZPA) cannot be achieved at this frequency therefore large circulating current can cause the degradation of efficiency. Authors in [136], investigated that there is always a trade-off between output voltage controllability and efficiency in order to get load-independent voltage gain using SS topology.

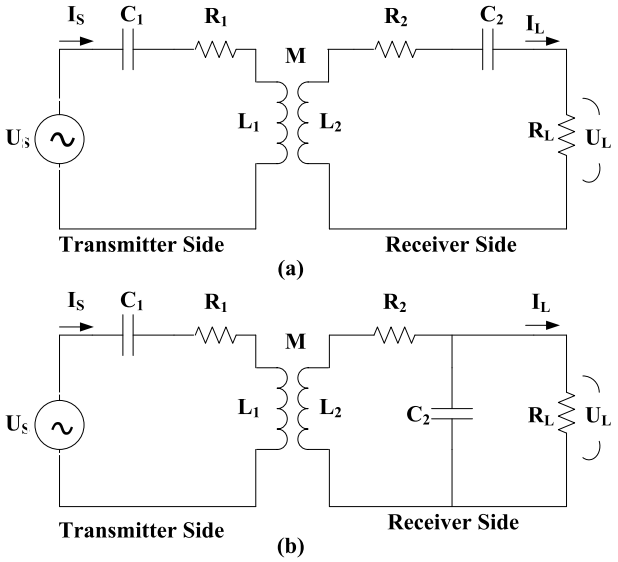

FIGURE 28. Equivalent circuit of (a) SS compensated network (b) SP compensation [136].

The combinations of two topologies using SS and PS for battery charging were proposed in [127]; however, two input sources, voltage source for SS and current source for PS were required, thus makes the system complex and uneconomical. Moreover, in [136], the authors have analyzed the SS compensation topology offers high efficiency and voltage gain, but it is sensitive to the output load changes and parasitic resistance. Therefore, in order to achieve maximum efficiency, the parasitic resistance of the coils at varying loads should be minimized. Moreover, the research reported in [138] and [139], found that the sensitivity of SS topology with respect to load variation can be improved by operating it around the frequency of load-independent voltage gain. But in this method, the ZPA operation is difficult to achieve thus causes the degradation of inverter efficiency.

B. SP COMPENSATION NETWORK

SP compensation topology as illustrated in Figure 28 (b), provides load-independent voltage gain with ZPA [140], suitable for high power applications [141]. However, SP compensation can give high efficiency when the load resistance is high, it is not suitable for the large disparity of coupling coefficient (k) due to misalignment or due to distance variations. Because in SP topology, the load-independent output voltage is inversely related to the k value [142]. Frequency domain analysis is conducted in [143] to study the SP topology, and a design method to achieve optimized quality factor (Q) is proposed using two cases, in first case LS1 $\leq$ LS2' and in second case LS1 > LS2'. Analytical equations are derived in both cases to achieve optimized Q for desired equivalent load resistance. It is proved that optimal Q value gives robustness in voltage and current gain without any significant increase in the circulating current of Tx and Rx coils.

C. PS AND PP COMPENSATION NETWORK

An equivalent circuit of PS and PP compensated system is depicted in Figure 29 (a) and (b). PS and PP compensation topologies are safe as compared to SS and SP during no load conditions, when Tx coil is ON and Rx coil is kept away from the Tx coil. However, during misalignment, these topologies affect the power transfer capability, because compensation capacitor values strongly depend upon the coupling coefficient and the load [144]. A comparative analysis of four compensations SS, SP, PS and PP performed [145], and it is found that SS and PS compensation performance was good for variable frequency operation. On the other hand, the performance of SP and PS was reasonable in the case of variable load and distances. However, it was noticed that PP compensation had very poor efficiency among all four topologies [145]. Moreover, it was analyzed in [144] that parallel compensation from primary side can be a good choice in the absence of receiver coil, however not appropriate in case of misalignment, because its capacitor compensation value strongly depends upon the coupling coefficient and output load, thus they are not able to transfer rated power.

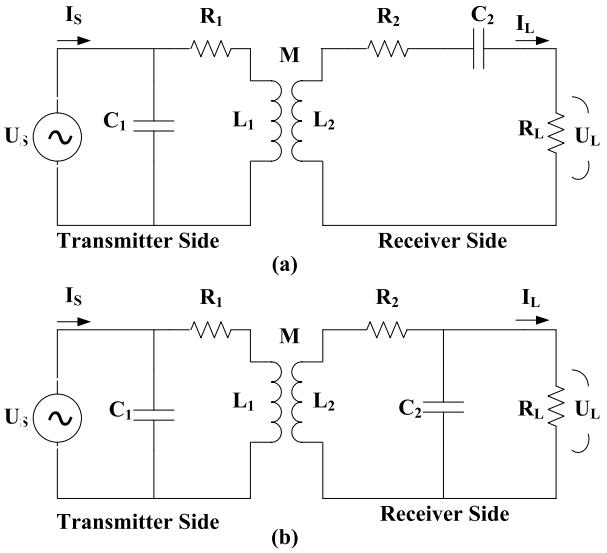

FIGURE 29. Equivalent circuit of compensated ICWPT system (a) PS (b) PP [144].

D. SP/S COMPENSATION NETWORK

A compensation utilizing series and parallel capacitors from the primary side and series capacitor from the secondary side is proposed in [146], as shown in Figure 30. This compensation is useful to maintain constant power during

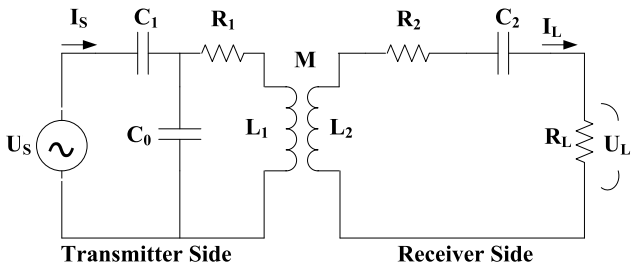

FIGURE 30. Equivalent circuit of SP/S compensated ICWPT system [146].

misalignment. It has the capability to maintain the desired power irrespective of coupling variation.

E. S/SP COMPENSATION NETWORK

Using series compensation from primary and series-parallel-combined compensation from secondary can be called as S/SP compensation, as shown in Figure 31. It provides the high efficiency and ZPA of input impedance along with load-independent voltage gain. However, it gives higher-order harmonics to the rectifier network, thus creates problems for rectifier filter design [147]. Moreover, it was also analyzed that the efficiency of S/SP compensation changes due to wide variation of coupling coefficient and misalignment, as the load-independent voltage gain is inversely proportional to the coupling coefficient.

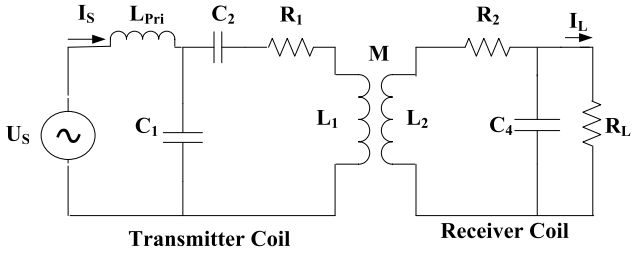

FIGURE 31. S/SP compensated ICWPT system [147].

F. A DOUBLE-SIDED LCC COMPENSATION NETWORK

LCC-LCC topology is shown in Figure 32, it was used by several researchers due to its high efficiency for electric vehicle battery charging [148], [149].

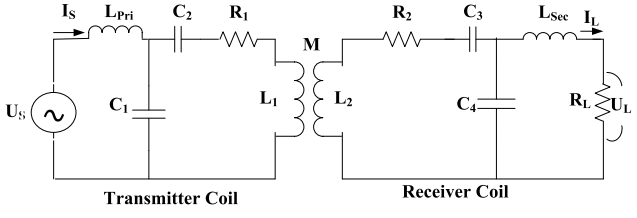

FIGURE 32. Double-sided LCC compensated ICWPT system [148], [149].

It was found that in case of heavy loads, the voltage stress on primary compensation capacitors is less in LCC topology than SS counterpart. However, it was difficult to achieve load-independent output voltage is difficult due to self-coupling between the compensation inductor and the main coil. When tuned properly, a resonant frequency which is independent of coupling and load can be obtained using double-sided LCC topology [103].

G. LCC-S COMPENSATION NETWORK

ICWPT system using LCC-S compensation was proposed in [22] for charging the battery of cardiac pacemaker, as shown in Figure 33. The power output of 3.072 W with an efficiency of 78.4% was achieved. LCC-S was also used for high power applications such as EV battery charging in. One kilowatt power was delivered to load with an efficiency of 94.8% with full load operation. However, the ZPA operation of input impedance, as well as load-independent operation was not discussed. A comparative study between LCC-S and SS is presented in [150]. Three parameters are focused for comparison, which is zero-phase-angle (ZPA), frequency and load variation with respect to power transfer performance of the ICWPT system. Moreover, the characteristics of voltage gain and input impedance angle under the conditions of ZPA frequency are also analyzed. and it is concluded that LCC-S is more suitable for low power applications, while SS is more feasible for high power applications. SS has higher load sensitivity to output characteristics than LCC-S.

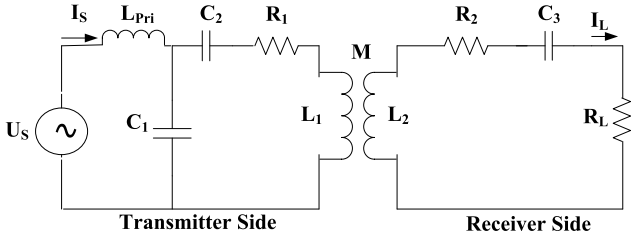

FIGURE 33. LCC-S compensated ICWPT system [151].

H. LCC-P COMPENSATION NETWORK

ICWPT using LCC-P compensation is shown in Figure 34 [152], which can provide load-independent constant current output. However, when secondary parallel compensation is used then a DC filter inductor (L0) is required. Therefore, a technique is proposed in [152] to eliminate the use of L0, thus the size of the secondary can be reduced. Moreover, a comparative analysis between LCC-P and SS is carried out based on output power and efficiency. It is found that LCC-P gives better efficiency than SS because of smaller conduction loss of inverter. The withstanding voltage of the receiver side capacitor (C2) without L0 is less around 40% compared to that with L0. The peak efficiency of 94% is achievable without L0, which is 1% less than that with L0. The withstanding voltage on C2 clamped to the battery voltage. It is found that

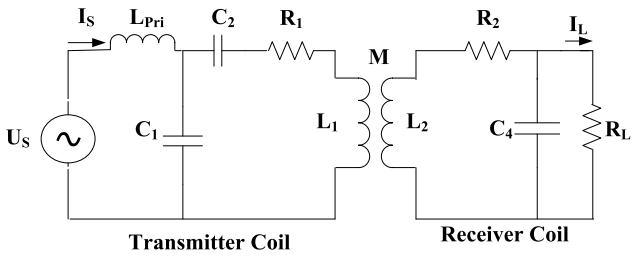

FIGURE 34. LCC-P compensated ICWPT system [152].

the output power is directly related to the battery voltage and the efficiency can be maximized by improving the voltage gain.

I. LCL COMPENSATION NETWORK

An inductor-capacitor-inductor (LCL) compensation was studied in [153], [154], and [155] which provides uninterrupted power, but it reflects reactive power back onto the source [156]. A tuning method for double-sided LCL compensation was proposed in [157], which provided slightly higher efficiency than the traditional tuning method; however, the constant current and voltage features were not studied. It is also known as the double-sided LC compensation network, because the last L can be ignored, because it corresponds to the Tx and Rx coil inductances as shown in Figure 35.

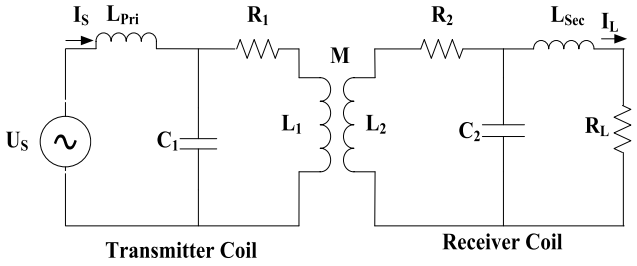

FIGURE 35. LCL compensation network [157].

Moreover, a comprehensive review of various compensation topologies focusing on bidirectional WPT system and its control mechanism is provided. The review covered the four fundamental compensations as well as hybrid compensations. Various control methods for bi-directional WPT technique were investigated such as the PID control, fuzzy logic control and sliding mode control etc. The applications of several compensations in bidirectional WPT method, their advantages, and limitations are also discussed [158].

Table 5 illustrates the summary of different compensation topologies. The power factor is less affected by variable frequency in the case of SS, PS, S/SP, and double-sided LCC topology. Moreover, the efficiency is less affected by frequency variations in the case of SP and PP topology. SS and SP compensation can provide maximum efficiency. However, load variation affects more on SP topology than SS. Load independent voltage characteristics are achievable using SS, SP, S/SP, and SP/S. However, PP, PS, and double-sided topology cannot give load-independent voltage characteristics. The table below shows the comparison of multiple compensation topologies.

The simplicity and safety of IPT technology [159] has several potential uses in portable devices [20], WSNs [160], IMDs [161], and electric automobiles [17]. To reduce the volt-amp (VA) rating of the source supply, it is generally advised to operate the primary-side inverter of IPT systems at ZPA. Additionally, the resonant inverter may operate at ZVS at ZPA with minimal electromagnetic interference (EMI) and switching losses [162], [163]. However, due to non-constant coil lengths, misalignment, shape deformation, or close contact to metal objects, it is frequently very difficult to sustain ZVS operation with variable couplings [20].

In Tables 6, all of the topologies' analytical findings are contrasted and compiled. Series-series (SS), SP, PS, and PP are the four fundamental compensation topologies [26], [144].

VI. TYPES OF COIL STRUCTURES USED IN ICWPT SYSTEM FOR ELECTRIC VEHICLES

A hexagonal coil structure of the receiver coil and circular structure of the transmitter is proposed in [164]. A planar coil structure for creating a three-dimension magnetic field around a cup is proposed in [165] for mobile phone charging [166]. In the case of EV charging, stationary charging coils are different from dynamic charging coils [167]. Usually, circular coils perform well for stationary EV charging. However, in case of dynamic EV charging, it was found that the overall performance of the ICWPT system is influenced by geometry of Tx and Rx coils, misalignment and load conditions [168], [169]. The Tx coils for dynamic EV charging are placed in long tracks [170] or in segmented tracks [171], [172] under the ground on the road. Dynamic EV charging can also be called as online electric vehicle (OLEV) charging. Different studies are presented to optimize the coil shapes [173]. The configuration of a long track transmitter is often kept longer than the EV length so that more vehicles can be handled at a time [174]. Usually, a long track transmitter system is supplied by a single source to make it simple and easy to control. The long track transmitter system proposed by the South Korean team of researchers [175], [176], for dynamic charging. This consisted of a high-frequency inverter, power factor correction (PFC) converter. In this system, power losses become high because the track of transmitters requires to be running all the time. Note that the radiation effect of the magnetic field needs to be further studied during the misalignment and during the unavailability of the receiver coil. To reduce the effect of magnetic field exposure in long track system, an "X" shape transmitter was suggested in [177]. Moreover, an additional coil was suggested along with the existing Tx assembly to mitigate the adverse effects of magnetic field radiation [178]. Besides,

TABLE 5. Summary of different compensation topologies and the load-independent operation.

Compensation Network	Maximum efficiency	Efficiency tolerance to variable frequency	Load-independent voltage output	Load independent current output
SS [137]	94.6%	Low	Directly related to coupling	Can be obtained at single resonance frequency, dependent on coupling coefficient.
SP [16]	94.6%	High	Inversely related to coupling	Can be obtained at lower or higher resonance frequency.
PS [145]	94.2%	High	Frequency and coupling dependent	Difficult to obtain.
PP [145]	94.3%	Low	Difficult to obtain	Frequency and coupling dependent.
S/SP [143]	93%	Low	Coupling independent	Difficult to obtain.
SP/S [147]	93%	Low	Coupling dependent	Difficult to obtain.
LCC-LCC [104]	93.5%	Low	Difficult to obtain	Can be obtained at single resonance frequency at fixed coupling coefficient.
LCC-S [152]	94.8%	Low	Can be obtained at single resonance frequency Coupling dependent	Can be obtained at higher or lower resonance frequency.
LCC-P [153]	94%	High	Difficult to obtain	Can be obtained single resonance frequency at fixed coupling coefficient.
LC-LC2 [135]	93%	High	Possible and less affected by coupling coefficient variations	Difficult to obtain

TABLE 6. Comprehensive comparison of the four fundamental topologies using various parameters.

Compensation	Z_T	I_t at Resonance	Z_{Ref} at Resonance	Characteristics output	Q_r	Q_t
PP	$\frac{1}{\frac{1}{\frac{\omega^2M^2(1+j\omega R_LC_r)}{Z_r(1+j\omega R_LC_r)}+Z_t}+j\omega C_t}$	$\frac{V_SL_r^2}{M^2R}$	$\frac{M^2R}{L_r^2}-\frac{j\omega_0M^2}{L_r}$	A source of current on the receiving end	$\frac{R}{\omega L_r}$	$\frac{\omega L_tL_r^2}{M^2R}$
SS	$\frac{\omega^2M^2}{Z_r+\frac{1}{j\omega C_r}+R_L}+Z_t+\frac{1}{j\omega C_t}$	$\frac{V_SR}{\omega_0M^2}$	$\frac{\omega_0M^2}{R}$	Receiving side from voltage source	$\frac{\omega L_r}{R}$	$\frac{L_tR}{\omega M^2}$
SP	$\frac{\omega^2M^2}{Z_r+\frac{R_L}{1+j\omega R_LC_r}}+Z_t+\frac{1}{j\omega C_t}$	$\frac{V_SL_r^2}{M^2R}$	$\frac{M^2R}{L_r^2}-\frac{j\omega_0M^2}{L_r}$	A source of current on the receiving end	$\frac{R}{\omega L_r}$	$\frac{\omega L_tL_r^2}{M^2R}$
PS	$\frac{1}{\frac{\omega^2M^2(1+j\omega R_LC_r)}{Z_r(1+j\omega R_LC_r)+R_L}+Z_t+j\omega C_t}$	$\frac{V_SR}{\omega_0M^2}$	$\frac{\omega_0M^2}{R}$	$\frac{V_SR}{\omega_0M^2}$	$\frac{\omega L_r}{R}$	$\frac{L_tR}{\omega M^2}$

an asymmetric design of the transmitter and receiver coils was proposed in [179] to increase the output power tolerance during the misaligned condition of coils. Furthermore, an extra quadrature coil was added to the asymmetric design of the receiver coil to further enhance the misalignment tolerance level [180].

A segmented track Tx based system was presented in [172] using a frequency of 85 kHz. The segmented track Tx size was around 1 m, which is compared with the same size of the long track Tx. It was found that the segmented track has higher efficiency than long track OLEV charging system. This is due to the low-quality factor of the long-guided track quality factor because of low efficiency of 20 kHz as compared to segmented track, which usually uses 85 kHz. In this research, the arrangement of segmented Tx coils was done in the form of an array of tracking lane.

Each Tx coil of the segmented track was equipped with its individual compensation circuit. In this way, the desired length of the segmented track was more convenient to design for powering the electric vehicles on the roadway. Moreover, a control system for segmented tracks was introduced in [181], to power ON and OFF particular Tx coils with respect to Rx coils. When Rx coil is not in the range of Tx coil, then it can be switched OFF automatically to reduce the losses of magnetic flux leakage. However, the design of segmented Tx coils is complex due to many numbers of compensation circuits and inverters, and control mechanism, hence, more cost is required for this type of configuration as compared to long-guided track Tx system.

The total cost of a segmented track can be decreased by sharing the same power electronic inverters in series or parallel. Another drawback of a segmented system was the power fluctuation due to the movement of the receiver coil. Moreover, in the segmented system, the transmitters are installed at a certain distance from each other to reduce the self-coupling and the number of transmitters. Therefore, in such system,

the power drops when receiver coil comes between two transmitters while during movement [181]. Power drop can be reduced by placing transmitters near to each other and then the self-coupling issue between two transmitters needs to be addressed. The author in [172] have suggested that the issue of self- coupling can be addressed by the optimized designs of Tx and Rx coils. In the case of stationary EV charging, the Tx coils are designed as a single coil from of segmented track. The single-coil used for stationary charging, when combined in a track with different types of arrangements can be used for dynamic charging as well [167]. There are several types of transmitter and receiver coils used for stationary and dynamic charging of EVs, such as circular, flux pipe, DD, DDQ, QDQ, and Bipolar.

A. CIRCULAR COIL STRUCTURE

The circular coil structure is non-polarized. Therefore, when the transmitter coil is circular then the receiver coil must be a circular shape. Otherwise many losses occur, because of significant flux leakage [72]. Circular coils offer a low height of flux path around one-fourth of the diameter of the coil, so coupling is not good enough [73]. The large diameter of a coil is required to produce good coupling between Tx and Rx coil. To transfer power through a large air gap using a circular coil is costly [66]. The circular coil as a transmitter generates the flux/field in a vertical direction only. To transfer a fair amount of power perfect alignment of the receiver coil is required. Therefore, Circular coils can be a good option for stationary charging applications. However, the circular coil structure is not appropriate for dynamic EV charging, because, during axial misalignment of around 38% power transfer becomes zero. Ferrite core can be used for improvement in the magnetic flux using circular coils. The layout of a circular coil structure along with ferrite core and aluminum shielding is illustrated in Figure 36. The aluminum shield is good for reducing the leakage of flux.

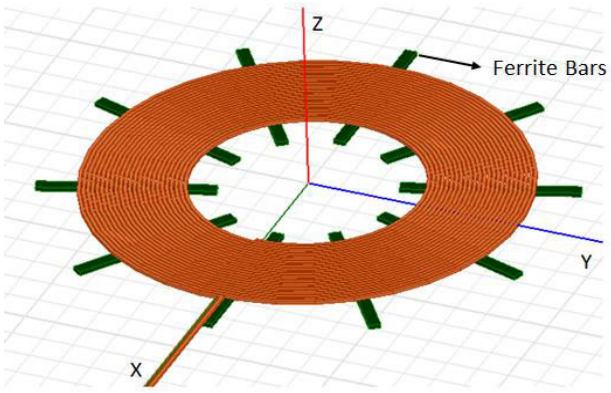

FIGURE 36. Circular coil with ferrite bars [66].

B. FLUX-PIPE COIL STRUCTURE

A flux pipe coil structure was proposed in [71], which was formed by a wounded coil along with an H-shaped ferrite bar, as shown in Figure 37. The flux pipe coil gives a higher flux path height than a circular coil. It provides flux path height around half of the coil length, thus reduces coil size and provides better axial misalignment tolerance than a circular coil. Flux pipe structure creates a double-sided flux path, where the non-useful flux is lost in the aluminum shielding set up behind the coil structure [182].

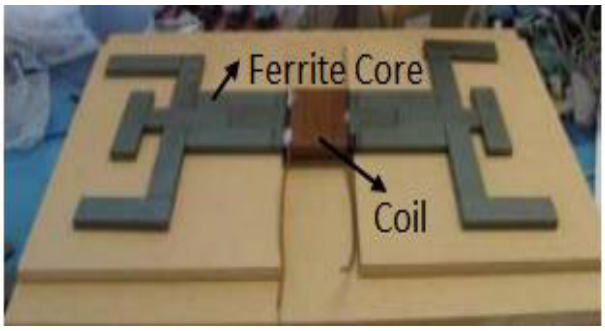

FIGURE 37. Flux-pipe pad [71].

C. DD COIL STRUCTURE

DD coil structure is proposed in [183], which is better than circular and flux pipe coil structure due to its single-sided flux path along with polarized behavior. DD structure is constructed two coils of ''D'' shape, as depicted in Figure 38. DD coil creates a horizontal field because of its polarized structure. The horizontal field produces good misalignment tolerance, thus coupling coefficient during axial misalignment can be improved. The height of the flux path of the DD structure is one-half of the length, like a flux pipe structure. The flux path height can be adjusted by changing the width of the overlapping area of the two ''D'' coils. DD coil offers an almost double charging zone than the circular coil. However, it also provides zero power transfer at horizontal misalignment of 34% like circular coil [183].

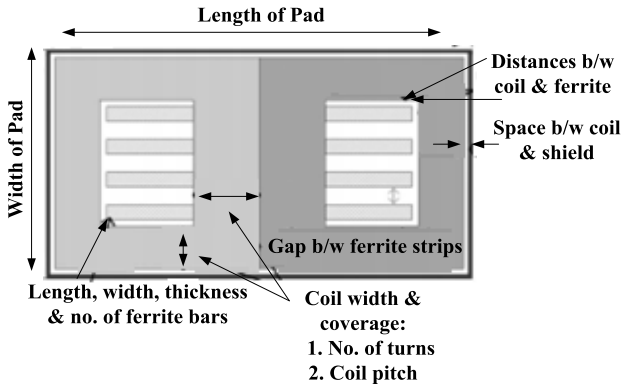

FIGURE 38. DD pads [183].

D. DDQ STRUCTURE

Figure 39 shows the layout of DDQ coil. This shape of the coil uses an extra D type coil, which is kept above the DD

coil at the overlapped region. When "D" coil placed over the DD coil at the center. The above "D" shape looks like Q, therefore this coil is named as DDQ coil [183]. It offers almost twice flux path height than circular coil along with an additional single-sided flux path. Although zero power transfer occurs at 77% of the horizontal misalignment, however, more copper is needed than other conventional coils [184].

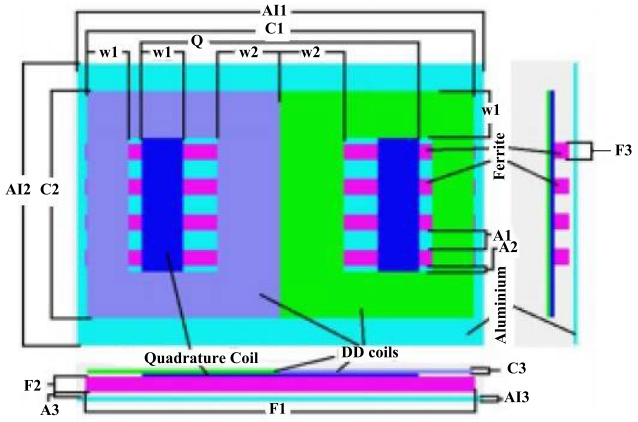

FIGURE 39. DDQ pads [184].

E. BIPOLAR STRUCTURE

The University of Auckland modified the design of the DD structure and proposed a new structure called bipolar structure [182], [184]. The used more size of D coil as compared to DD shape and created an overlap between two D coils, as shown in Figure 40. This pad performance is identical to a DDQ structure, and it uses less amount of copper than DDQ pad.

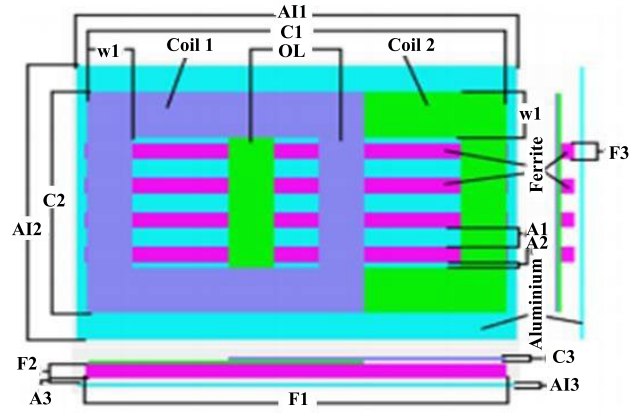

FIGURE 40. Bipolar pad [184].

F. COMPARISON OF DIFFERENT COIL STRUCTURES FOR EV APPLICATIONS

EV systems use many coil structures for EV charging applications. Among them, circular is most common. Apart from that, DD, DDQ, bipolar are also widely used coil structure pad. The circular structure is good for stationary charging applications because it has very poor misalignment tolerance due to less flux path height. While DDQ and bipolar structures give good misalignment tolerance because it has a minor effect of power transfer fluctuations during misaligned conditions. Table 7 provides a comparison of different coil structures.

VII. RECENT RESEARCH ON ICWPT TECHNOLOGIES

ICWPT technology is now being improved in terms of power transfer efficiency (PTE) and lengthening the distance between Tx and Rx by numerous academic and industrial researchers. The researchers are also interested in the misalignment of the Tx and Rx. The misalignment between Tx and Rx can greatly reduce the efficiency of power transfer, as shown in [185]. For a multi-dimensional ICWPT structure, a thorough description was provided in [186]. Additionally, as was noted in [118], the frequency splitting phenomena frequently occurs in the system architecture with many relays, transmitters, and receivers coils when two or more resonant coils are close enough to one another for their magnetic fields to be reasonably strongly coupled. A novel ICWPT circuit with magnetic dipoles with optimum-stepped core structures was presented in [187], as illustrated in Figure 41, and the results are displayed in Figure 42. This circuit is operated by an inverter with a 20 kHz switching frequency. The achieved efficiencies at 3, 4, and 5 meters away were 29%, 16%, and 8%, respectively, with output powers of 1403, 471, and 209 W.

Due to its geometrical design and ability to be set in a room's corner, the proposed coil can only be effective as a transmitter coil. Due to its bulk and long shape, this sort of coil is very challenging to utilize as a receiver. Additionally, it was determined that the radius and quantity of coil turns are connected to the maximum distance between Tx and Rx. To increase transfer efficiency using frequency ranges from 100 kHz to 20.1 MHz, a circuit model was created and the ideal spacing of the coils were deduced analytically. Maximum power transfer efficiency was attained at 14.6 MHz frequency in [189]. As seen in Figure 43, the authors of [190] proposed the notion of combining a traditional source resonator with an extra resonator whose resonance frequency is higher than the magnetic field excitation frequency. The installation of this second resonator increased the power transmitter's magnetic dipole moment and effective permeability by producing a significant paramagnetic response.

Further research revealed that the resonance frequency of the additional resonator may be changed to control effective permeability, and that higher effective permeability results in larger resonant coupling at the same excitation amplitude. By utilizing this technique, the power transferred to the load increased from 0.38 W to 5.26 W while maintaining the same excitation voltage of 10 V, improving the transfer efficiency from 57.8% to 64.2% at a distance of 15 cm. Figure 44 illustrates a unique concept of two tightly linked resonators utilizing four coils that was proposed in [191].

TABLE 7. Comparison of different conventional coil structures.

Coil Structures	Flux path height	Misalignment Tolerance	Zero Power Transfer Zones with horizonal offset
Circular Coil	1/4 of the coil's diameter	Misalignment tolerance is not so good, but good for aligned conditions	Occurs at about 38% of the coil diameter [188]
DD Coil	1/2 of the coil's length	Good tolerant in the y-direction	Appears at about 34% of the coil length [183]
DDQ Coil	2 times of circular coil with an extra single sided flux path	DD coil provides good tolerant in y-direction and Q coil provides good tolerant in x-direction	Appears at around 77% of the coil length [184]
Bipolar Coil	2 times of circular coil	Good tolerant in both direction	Same as DDQ coil [184]

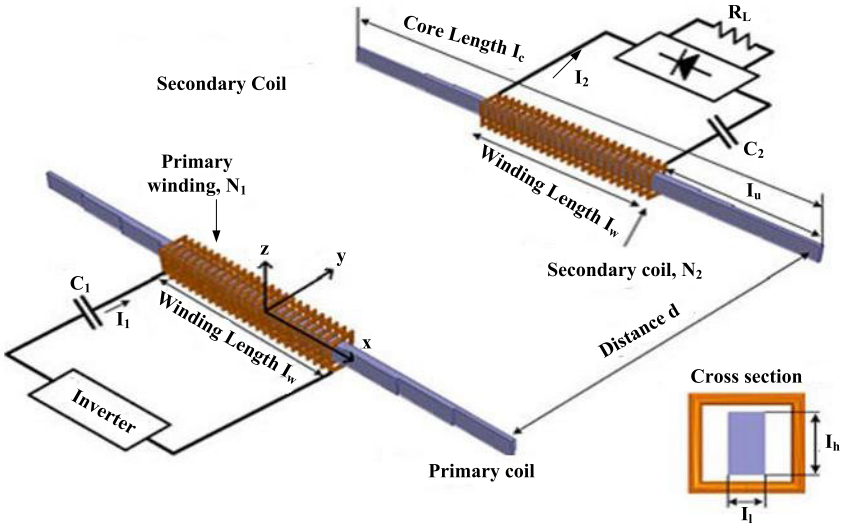

FIGURE 41. Proposed Inductive Power Transfer System in [187].

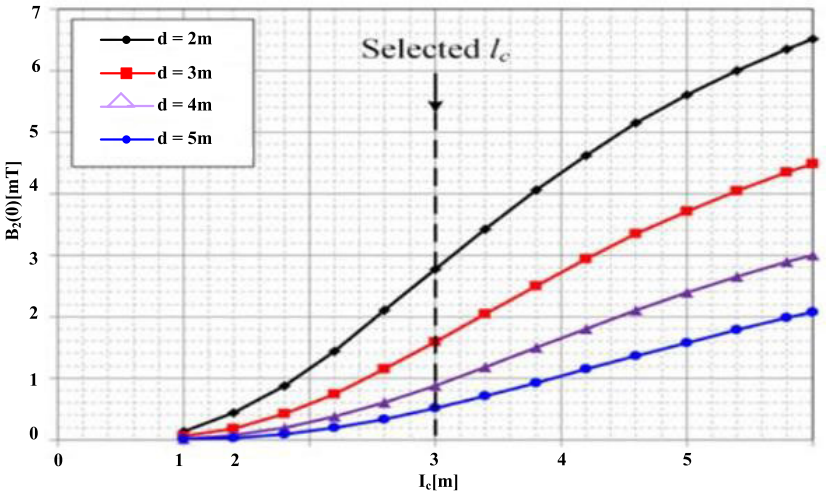

FIGURE 42. Results of the magnetic flux density simulation for the main and secondary core lengths LC (1-6 m) and different distances d (2-5 m) at the center of the secondary coil. Design with LC = 3 m was chosen as the standard [187].

In contrast to the usual four-coil type, it also includes the first and fourth coil in a strong cross-coupling with a high Q. It was shown that the proposed model has an efficiency of 65.2% and a power transmission of 17.2 W at a distance

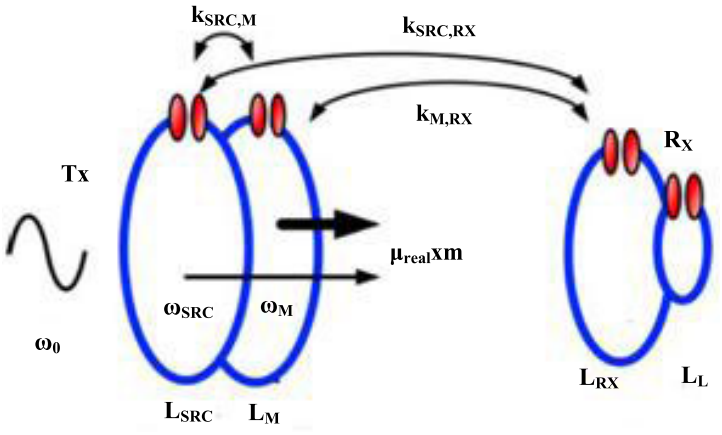

FIGURE 43. Conventional four coils structure with additional resonator (LM) [190].

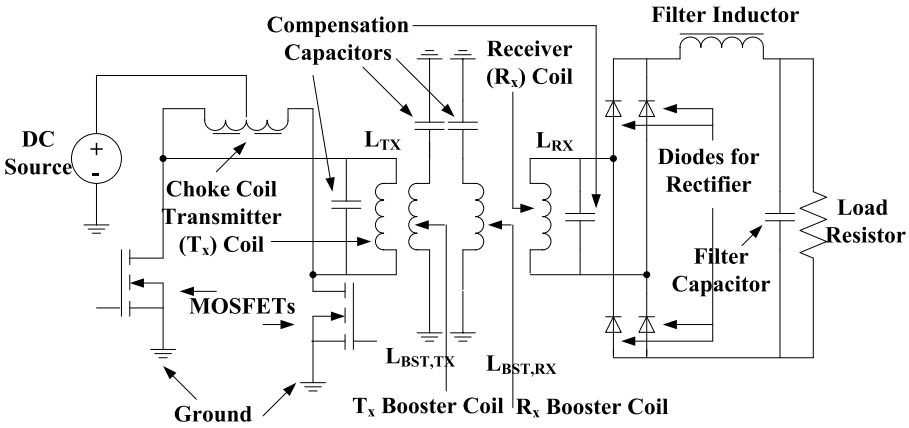

FIGURE 44. Schematic diagram of four coil resonator using MOSFET [191].

of 13 cm, compared to figures of 37.3% and 6.2 W for the standard four coil approach at the same distance. Additionally, [192] presented an efficiency analysis of a WPT system with a typical four coils and an intermediate resonant coil, as shown in Figure 45.

To reduce the volume of the intermediate coil, a spiral coil was used. The source and load coils were made of two single turn coils, while the Tx and Rx coils were made of helical coils. This layout was able to boost efficiency and the distance between Tx and Rx, but the intermediate coil and its control raised the system's overall cost. The intermediate coil was set up both coaxially and perpendicularly, but the former configuration was far more effective. However, the perpendicularly oriented intermediate system may be preferable from a practical standpoint because it can be implemented in the space designated for wall-mounted TVs and furniture embedded systems. Circuit theory was used in [193] to analyses the frequency splitting phenomenon of the two-coil and three-coil RCWPT systems in detail.

It was determined that two splitting frequencies, 9.5 MHz and 10.5 MHz, happen when the coupling coefficient is large enough. To choose the best frequency for optimum power transfer, the magnetic field distribution of the two splitting frequencies was also simulated and examined. Additionally, the critical coupling coefficient of the two- and three-coil ICWPT, which establishes the over coupled zone, was determined. Finally, a tuned frequency technique was suggested in light of the numerical outcomes. Furthermore, a fresh approach called ''frozen resonance state'' was presented in [194] for dynamically matching the resonant frequency without changing the values of the constituents.

Table 8 presents a summary of recent work in ICWPT technology. The table is summarized in terms of resonance frequency, efficiency, distance, and power level in order to understand the overall performance of various ICWPT models.

A. HUMAN EXPOSURE BASED INDUCTIVE POWER TRANSFER SYSTEM

The assessment of the human body's exposure to stray electromagnetic fields produced by WPT devices is a crucial problem that could restrict the use of this technology in

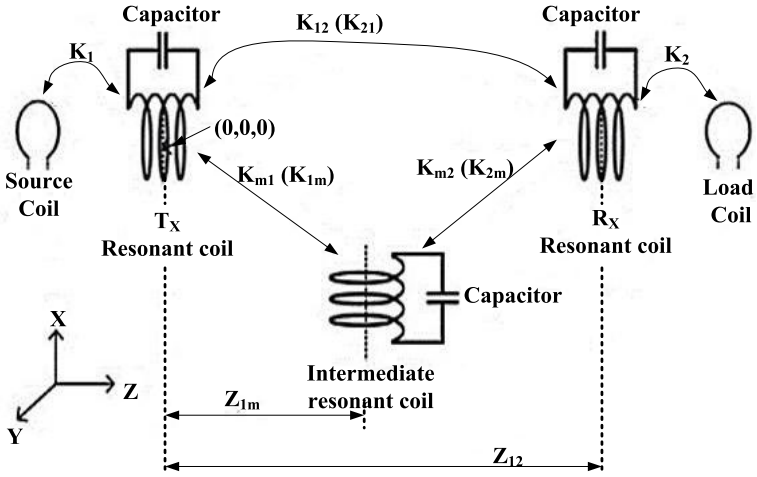

FIGURE 45. Structure of four coil resonators using intermediate coil [192].

TABLE 8. Recent work in WPT technology.

Ref	Frequency	Power, Voltage, Current	Distance/ Coupling Coefficient (k)	Inductance (µH)	Efficiency	Comments
[18]	10 MHz	60 W	2 m	NA	40%	Use 4 coils Wires with a very high quality factor (Q=950) are utilised with a very high frequency.
[20]	10 MHz	12 W	70 cm	L1=L4= 1 L2=L3= 20	50%	4 coils used, Coefficient of determination (R2) of 0.9875 between measured and calculate values.
[84]	4 MHz	4.835 V, 0.048 mA	10 cm 20 cm	L1=L2= 4	85% 45%	2 coils use the diameter of coil and transmission distance is same, that is the reason behind high efficiency. Series parallel mixed topology used.
[195]	144 kHz 149 kHz	51 W to 65 W	0.025-0.063	Tx1=Tx2=39, and Rx1=44, Tx1=1, Rx1=Rx2=99	45% to 57%	Multiple coupling effect investigated. In first case 2 transmitters 1 receiver used and in second case 2 receivers and 1 transmitter used.
[196]	13.56 MHz	PF =50 W, Efficiency=PL/PF, PL is not given.	15 cm	L1=L2=7.8	73% and 66%	High frequency used. Efficiency of 73% with resistive load and 66% with battery is achieved.
[191]	200 kHz	17.2W	13cm	NA	65.2%	4 coils used. 2 transmitters and 2 receivers of same inductance value. High quality factor coils used.
[190]	13.56 MHz	5.26 W	15cm	L1=0.31, L2=1.97 L3=1.52, L4=0.344	64.2%	4 coils used. Good for low power applications
[197]	6.78 MHz	2 W	40 cm	L1=1.33, L2=40.1 L3=39.5, L4=1.35	74%	4 coils used. The model tested for 60% Angular Misalignment and efficiency is good, but coil quality factor is very high.
[187]	20 kHz	209 W 471 W	5 m 3 m	L1=L2= 942	8% 29%	2 coils of very high inductance used, and the frequency is also low in kHz range.
[97]	500 kHz	1 W to 10 W	13 cm	L1=40, L2=58.1 L3=60.3, L4=40	80%	4 coils used. Tx coil (L2) to Load coil (L4) efficiency around 80%. Source and load coils replaced by impedance transformers.
[198]	164.76 kHz	0.151 W, 3.02 V, 50.01 mA	50 cm	L1=L2= 100	25.2%	Input 12 DC, 0.5 A. Inductor size quite large made with copper tubing. Efficiency is low.
[192]	85 kHz	3 kW	15 cm	L1 = 225.35, L2=159.45, Lf1=46 and Lf2=38	95.5 % (dc-dc efficiency)	Integrated LCC topology used. Input voltage was 330 V.

daily life. An anatomical human model and a homogeneous ellipsoid phantom exposed to a WPT system prototype with a power of 560W, which was previously experimentally characterized, underwent a numerical dosimetric investigation to assess the electric (E) field created [199]. Furthermore, the ferrite to chassis distance is 0.5 cm, and the coil-to-coil distance is 15 cm. On a 400 V battery, the system is expected to deliver 3 kW (typical charging). This charging mechanism has a chosen frequency of 30 kHz [200]. An assessment is made of the magnetic field that a wireless WPT system

emits when a small EV is being statically charged [201]. The procedure and finding for evaluating how much a person is exposed to a magnetic field when using a real IPT installation. A 20 kW IPT system for a light commercial vehicle running at an 85 kHz frequency is the subject of the case study. The dynamic charge is carried out via a number of separate transmitters that are only turned on when the vehicle passes over them. Each transmitter measures 0.5 m in width and 1.5 m in length [202].

However, International Commission on Non-Ionizing Radiation Protection (ICNIRP) advises that the average allowable exposure of humans to the electromagnetic field must be below 27 μT to support our proposed study [203], [204], [205]. Furthermore, ICNIRP published Guidelines in 2020 for protection of humans from exposure to electromagnetic fields from 100 kHz to 300 GHz. These revised guidelines supersedes the previous guidelines provided by ICNIRP in 1998 and 2010, respectively [206], [207].

Additionally, this paper proposed the operating conditions for the estimation of the induced electromagnetic field from transmitter to receiver coil in inductive power transfer system. Numerical modeling is performed of standing human model for understanding the electromagnetic field exposure in nearby vicinity of transmitter coil [200]. Moreover, the concerns regarding safety standards of the electromagnetic fields during wireless charging of EVs are deliberated. Furthermore, a methodology for the assessment of the human exposure to magnetic fields generated by dynamic wireless charging of EVs is proposed for evaluation of peak exposure by means of a time-harmonic formulation [202]. In this regards, instead of the permissible external field level a new assessment method based on the emitted field strength evaluation for wireless charging of EVs is implemented. The post-processing of the internal electric field, based on the IEEE C95.1 standard-2019, is discussed for taking in account the impact of skin-to-skin contact. This standard is more suitable for practical scenario and compliance assessment is simpler than the conventional approach [208]. ICNIRP published Guidelines in 1998 for human exposure to time-varying EMFs up to 300 GHz. Thereafter, due to considerable development in addressing the relation between radiofrequency EMFs and adverse health outcomes, the ICNIRP has updated the EMF guidelines for human safety in 2020 [207]. This study evaluates the human exposure to magnetic field specifically for static wireless charging of compact EVs. The realistic human model was considered in different positions inside and outside the charging vehicle. The misalignment condition between transmitter and receiver coils was also considered in this study. It was concluded that the reference levels surpassed in the case of lying position on the floor with hand nearby the coils [201].

B. BATTERY CHARGING ENERGY REQUIREMENTS FOR EVS

The amount of energy an EV needs depends on its SOC upon arrival. This energy, which is needed to finish the battery's complete charge and is expressed as:

$$E_r = \frac{(1 - SOC_a) B_C}{\eta} \tag{1}$$

where E_r represents the energy needed to fully charge the battery, B_C represents battery capacity, and represents the EV's charging efficiency. Efficiency for an electric vehicle (EV) in charging mode is $\frac{1}{\eta_C}$, and efficiency for an EV in discharging mode is η_d [209].

C. MODEL FOR THE LOWEST CHARGING/DISCHARGING COST

The price of charging and discharging affects the overall expense borne by the CC. The entire cost will be made up of the costs associated with charging, revenue from charging, and battery deterioration costs. The charging and discharging cost is written as follows:

$$C_{Ch\arg e} = \sum_{i=1}^{Nv} \sum_{t=1}^{ti,p} \lambda^t x \tag{2}$$

where,

λ^t is electricity price at time t

x is charging/discharging rate at time t as define below:

$$x \begin{cases} x_{ch}^t \eta_C & ch \arg ing \bmod e \\ \dfrac{x_{dch}^t}{\eta_d} & disch \arg ing \bmod e \end{cases} \tag{3}$$

Here

$x > 0$ represents charging mode while $x < 0$ signifies discharging mode. $t_{i,p}$ is parking duration of i^{th}EV. Battery degradation cost is expressed as [210] and [211].

VIII. PERFORMANCE PARAMETERS OF ICWPT SYSTEM

Following are some important performance parameters of ICWPT system.

A. COUPLING COEFFICIENT AND QUALITY FACTOR OF THE COILS

The coupling coefficient measures the air gap between Tx and Rx coil, when $k \geq 0.5$, it means a tightly coupled transformer with no air gap or very small air gap between Tx and Rx. When $k \leq 0.5$, it indicates that loosely coupled transformer, such as the ICWPT system, where coupling between Tx and Rx is loose with some air gap in centimeters. When k=0, it means there is no mutual inductance between Tx and Rx, so no power can be transferred. The value of M and k depends on the dimensions and number of turns of the coil and the distance between the coil. If the coil is wound on the core, then k value also depends upon the magnetic properties of the core material. The reduction of k value occurs due to misalignment and distance variation between the coils. The efficiency is directly proportional to the coupling coefficient, therefore, is it easily affected by misalignment and distance variation between the coils. The quality factor can be defined by the inductance of the coil. If the coil is more inductive, and

very less resistance, then it can offer higher quality factors. High-quality factor material can be good transferring power from Tx to Rx over a certain distance because it offers enough magnetic field path to transfer the power.

B. TOLERANCE ABILITY TO MISALIGNED CONDITIONS

When the receiver (Rx) coil is not properly aligned with the transmitter (Tx) coil, then efficiency can be reduced due to power transfer fluctuation. Lateral (horizontal) and longitudinal (vertical) misalignment between Tx and Rx coil directly affects the efficiency and power transfer capability of ICWPT system [136], [146]. Therefore, in case of EV charging system, higher misalignment tolerance is required to avoid the decrease of efficiency because of inaccuracy of electric vehicle parking. The precise alignment can decrease the leakage flux, consequently, reduces the intrusion of electromagnetic emission from the system.

Lateral misalignment occurs when the horizontally not aligned, while longitudinal misalignment occurs due to the instability of coils with respect to their lengths [168]. Design of coil structure as well as compensation topology can play a vital role the reduce the adverse effects of misalignment [146]. By selecting proper coil structure and compensation network, the power transfer capability during misalignment can be increased.

1) MISALIGNMENT BETWEEN THE COUPLED COILS

The power transfer efficiency and the amount of power that may be transferred are both greatly reduced by the axial and angular misalignment between magnetically connected coils in an ICWPT system. The primary coil driver operates in an unturned condition as a result of coil misalignment, which results in subpar switching operations and an increase in switching losses [65]. To reduce the negative consequences of misalignment between the magnetically connected coils, it would be helpful to investigate the tuning mechanism. In this research, the investigation of the tuning method by adjusting the duty cycle of the MOSFET gate driving signal, while maintaining the constant frequency of the MCR model will be conducted. Multiple case studies related to ICWPT technology.

C. OPERATING FREQUENCY SELECTION

The selection of frequency depends upon the desired power output. Usually, for high power applications, frequency is kept from 20 kHz to 200 kHz. Using high frequency, more power can be transferred. But it is difficult to create high power high-frequency supply due to the limited speed of high-power inverters. In the case of low-power applications, the switching speed of inverters in MHz is achievable. Moreover, the AC resistance is directly proportional to the frequency. As the frequency increases, the resistance increases because of skin effect. High efficiency is achievable using the high-quality factor coils and improving the coupling coefficient. The coupling coefficient can be improved by designing and analyzing the different coil structures. Ferrite core can also be used along with the coil to improve the coupling coefficient. The quality factor can be enhanced by using a high-frequency supply, therefore optimal frequency selection is important. The inductance of the coil depends upon the shape of the coil. Lawrence Berkeley Laboratory used the frequency of 180 Hz only for an electric highway system in 1978; however, it requires a huge inductor coil size because of low frequency [87]. Thereafter, researchers of the University of Auckland increased the frequency to 20 kHz [187], [212], which reduces the weight of the Tx and Rx coil, however, efficiency was still not so high. Then a frequency of 30 kHz used in 2010 by Korean researchers and they managed to get efficiency between 70-80%. Society of Automotive Engineers (SAE) has selected the operating frequency of 80-90 kHz while keeping the exposure limit of the electromagnetic field under safety for high power applications this frequency is widely used for wireless charging of EV applications. Bosshard et al. utilized the operating frequency of 85 kHz and managed to achieve an efficiency of 95.8 % in 2016 [93].

D. FREQUENCY SPLITTING PHENOMENON

The frequency splitting issue significantly affects the ICWPT system's output power. It causes the efficiency of electricity transfer to decline. If the coupling coefficient of two or more nearby resonant coils is big enough, this phenomenon can occur in a single or many transmitter and receiver coils. Impedance matching or adaptive frequency shifting is a typical strategy to address this problem. But in [118], the authors looked at the splitting mode for transmission in a single-transmitter, multiple-receiver resonant system and used the frequency splitting as a beneficial occurrence for many receivers in straight domino-resonators. In [193] authors claim that the multiplicity of the splitting frequencies depends on the fluctuation of the distance between the transmitter and receiver within the range below the critical point. The input impedance changes to tiny amplitude with an increased impedance angle and the frequency separates into two peak values. The splitting frequencies were also found to be different from the natural resonant frequency. These could be either greater or smaller than the natural resonance frequencies. The odd mode corresponds to the lower of these two splitting frequencies, and the even mode to the higher. Therefore, the ideal mode for obtaining greater efficiency was designed and researched using the frequency control system. The critical coupling point, beyond which efficiency significantly declines, is the coupling point at which the highest power transfer efficiency may be obtained. The over coupled regime is depicted in Figure 45 highlighted red volume, where frequency splitting takes place and transfer efficiency can be maintained regardless of distance if the right frequency is selected [81].

Figure 46 shows that maximum power transfer (S21 magnitude) works on only single resonant frequency during

critical coupled and under-coupled condition when it crosses through the critical coupling point and enters in over coupled region, it bifurcates into peaks. A method to avoid frequency splitting for biomedical implants using tunable LC compensation from the primary side was proposed in [110].

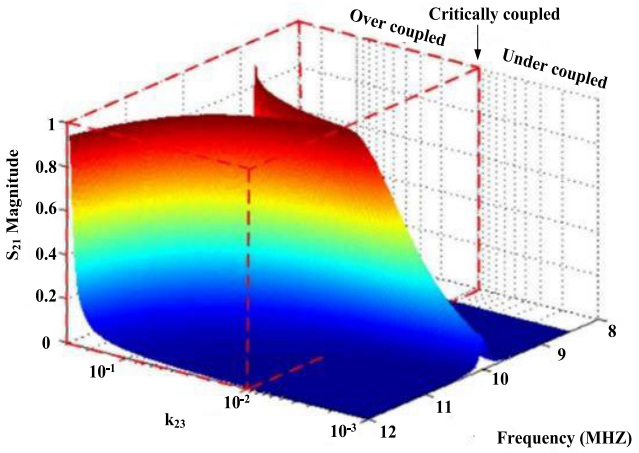

FIGURE 46. S21 magnitude for the simplified circuit model as a function of frequency and transmitter-to-receiver coupling k23 [20].

It showed that when two coils are over the coupled region, frequency splits in two peaks, then LC tuning can be useful to avoid frequency splitting phenomenon. A genetic algorithm-based tunable selection of LC network was proposed using high frequency of 13.56 MHz. However, these types of tunable matching networks are very difficult to implement in practical high-power applications, since many combinations of different inductors and capacitors for tuning according to desired value. Apart from that switch losses also occurs during. Therefore, tunable impedance matching can only be suitable for low power applications.

E. CONTROL METHODS

Different control methods were investigated for ICWPT systems. Some researchers suggested the control from the primary/transmitter side [172], [213], while others investigated the secondary side control [214]. Dual side control also investigated in [63]. In the case of single transmitter and single receiver, the primary side and dual-side control are appropriate options. However, in the case of multiple receivers powered by a single transmitter, a secondary side control can be used. Investigation of primary side control can be done by a phase shift, duty cycle adjustment, and frequency variation. Secondary side control can be achieved by applying buck or boost converter, MOSFETS, diode or DC inductor after the rectifier. Closed-loop control system can be also implemented by getting the information from secondary side and controlling from the primary side. Dual-side control system requires higher cost due to its complexity and implementation from primary and secondary side simultaneously; however optimal efficiency can be achieved.

F. SOFT SWITCHING AND HARD SWITCHING

Soft switching can be defined as the achievement of smooth voltage/ current transitions during the switching moment. Hard switching is contrary to soft switching, it means that switching the inverter driver circuit at any moment in time without taking care of the smooth voltage/current transition as illustrated in Figure 47 [215].

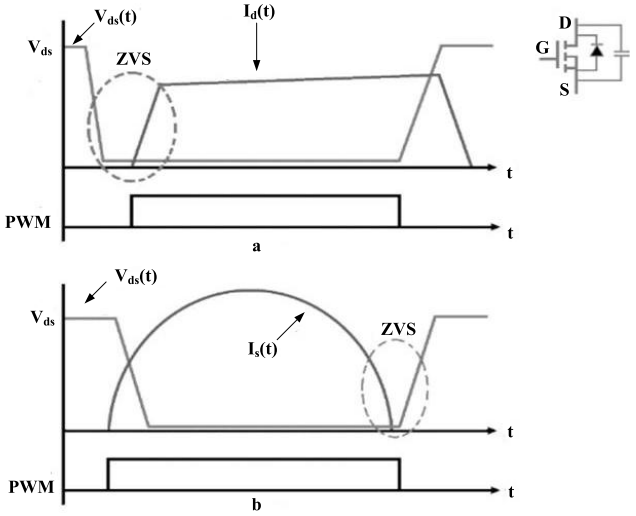

FIGURE 47. Voltage, Vds and current, Id waveforms in MOSFET for (a) ZVS (b) ZCS [216].

In other words, hard switching depends upon the ability of device with outside interference. However, to achieve soft switching, external lumped elements, i.e. inductors and capacitors need to be added. Another way of soft switching is to control the voltage and current time to minimize the intersection of their waveforms. Mostly metal oxide semiconductor field effect transistor (MOSFET) is used for inverter driver circuit of ICWPT system to create HF-AC supply. To reduce the switching loss of the inverter, soft switching is preferred; it includes the zero-voltage switching (ZVS) and zero current switching (ZCS). ZVS can be defined as the switching the inverter, when voltage is zero. To reduce the switching loss, it is preferable to switching on and off all the MOSFETS of the inverter at ZVS. Besides, ZCS is defined as the switching the inverter when current is zero. ZCS is not a perfect soft switching in inverter containing MOSFETSs and diodes [103]. It can induce high voltage stress on the parasitic capacitance of MOSFET before turning-on transition.

Therefore, it causes high switching losses and consequently decreases the inverter lifespan [216]. To realize soft switching for power electronics converters, the primary side compensation network is tuned in a way that it has a small portion of reactive power to reach ZVS or ZCS. Eventually, the parameters for realizing ZVS and ZCS become close to the parameters of ZPA [17]. Theoretically, ZPA can be defined as the in-phase behavior of input voltage (output voltage of the inverter) and the input current (output current

of the inverter). However, in practice, the input impedance should be slightly inductive to smoothly achieve ZVS of the MOSFETs to minimize the switching losses [217].

IX. CONCLUSION

This article initially presented the historical background of WPT technology. From the comprehensive literature review it was discovered that two main methods of WPT system are prominent, which are recently used by many researchers, these are inductive coupled wireless power transfer (ICWPT) and resonant coupled wireless power transfer (RCWPT). It was further extracted that RCWPT uses higher frequency in MHz range and suitable for low power applications. Moreover, ICWPT system is more suitable for high power WPT applications. The comparison between low power and high-power technologies is also provided in this review paper. Besides, several methods for analyzing and designing an appropriate WPT system are also presented in this review. These methods include the circuit analysis technique via mathematical equations, suitable software for circuit simulations, and software for 3D coil design etc. Besides, the different compensation topologies for ICWPT are analyzed and their load-independent operation is discussed. Furthermore, the design of wireless charging coils for electric vehicle application is also reviewed. Frequency splitting phenomenon and other related performance parameters of WPT system are provided in this review paper to enrich the understanding of reader. Moreover, safety standard for ICWPT technology are also discussed in this review paper. Overall various impactful literature studies have been included and referenced in this chapter to enrich the understanding of the readers. The importance of quality factor of coils and their impact on efficiency using different compensation topologies is also covered in this review.

WPT has been applied in numerous applications up to this point. The toothbrush, electric car, and mobile phones and their accessories are some of the most well-known uses. The potential for WPT to power drones or Internet of Things gadgets like security cameras. The medical industry is one sector where WPT technology is very interested. Brain simulators are one of those applications in the medical areas. The design of an additively made coil for various WPT topologies and coil shapes will be assessed in the future. The very constrained operating frequency spectrum that is typically required for receiver inductive coupling wireless power transfer (RICWPT) systems in industrial applications makes it challenging to employ this method. Additionally, the impact of changing the diameter of the coil the mutual inductance coefficient, and the distance between the coils on parameters like the self- and mutual inductance of connected coils, which is crucial in WPT applications. The study's encouraging findings demonstrate the great potential of wireless power transfer to address a variety of current industrial issues.

AUTHOR CONTRIBUTIONS

Masood Rehman, Sohrab Mirsaeidi, Nursyarizal Mohd Nor, Mohsin Ali Koondhar, Muhammad Ammirul Atiqi Mohd Zainuri, Zuhair Muhammed Alaas, Elsayed Tag-Eldin, Nivin A. Ghamry, and M. M. R. Ahmed have contributed to the design and implementation of the research, to the analysis of the results and to the writing of the manuscript.

CONFLICT OF INTEREST

Author has no conflicts of interest to disclose.

REFERENCES

[1] S. Y. R. Hui, W. Zhong, and C. K. Lee, "A critical review of recent progress in mid-range wireless power transfer," *IEEE Trans. Power Electron.*, vol. 29, no. 9, pp. 4500–4511, Sep. 2014.

[2] R. H. S. Yuen, "A critical review of recent progress in mid-range wireless power transfer," *IEEE Trans. Power Electron.*, vol. 29, p. 9, 2014.

[3] N. Tesla, "Apparatus for transmitting electrical energy," U.S. Patent 1 119 732, Dec. 1, 1914.

[4] C. Gerekos, "The Tesla coil," Phys. Dept., Université Libre de Bruxelles, Brussels, pp. 20–22, 2012.

[5] W. C. Brown and E. E. Eves, "Beamed microwave power transmission and its application to space," *IEEE Trans. Microw. Theory Techn.*, vol. 40, no. 6, pp. 1239–1250, Jun. 1992.

[6] J. O. McSpadden and J. C. Mankins, "Space solar power programs and microwave wireless power transmission technology," *IEEE Microw. Mag.*, vol. 3, no. 4, pp. 46–57, Dec. 2002.

[7] W. Brown, "Experiments in the transportation of energy by microwave beam," in *Proc. IRE Int. Conv. Rec.*, 1966, pp. 8–17.

[8] J. Benford, "Space applications of high-power microwaves," *IEEE Trans. Plasma Sci.*, vol. 36, no. 3, pp. 569–581, Jun. 2008.

[9] G. Chattopadhyay, H. Manohara, M. Mojarradi, T. Vo, H. Mojarradi, S. Bae, and N. Marzwell, "Millimeter-wave wireless power transfer technology for space applications," in *Proc. Asia–Pacific Microw. Conf.*, Dec. 2008, pp. 1–4.

[10] A. P. Sample, D. J. Yeager, P. S. Powledge, A. V. Mamishev, and J. R. Smith, "Design of an RFID-based battery-free programmable sensing platform," *IEEE Trans. Instrum. Meas.*, vol. 57, no. 11, pp. 2608–2615, Nov. 2008.

[11] P. E. Glaser, "Power from the sun: Its future," *Science*, vol. 162, no. 3856, pp. 857–861, Nov. 1968.

[12] C. E. Greene, D. W. Harrist, and M. T. McElhinny, "Powering cell phones and similar devices using RF energy harvesting," U.S. Patents US20 090 102 296 A1, Apr. 23, 2009.

[13] H. Zheng, K. Tnay, N. Alami, and A. P. Hu, "Contactless power couplers for respiratory devices," in *Proc. IEEE/ASME Int. Conf. Mech. Embedded Syst. Appl.*, Jul. 2010, pp. 155–160.

[14] J. Sallan, J. L. Villa, A. Llombart, and J. F. Sanz, "Optimal design of ICPT systems applied to electric vehicle battery charge," *IEEE Trans. Ind. Electron.*, vol. 56, no. 6, pp. 2140–2149, Jun. 2009.

[15] J. C. Schuder, "Powering an artificial heart: Birth of the inductively coupled-radio frequency system in 1960," *Artif. Organs*, vol. 26, no. 11, pp. 909–915, Nov. 2002.

[16] W. Zhang, S.-C. Wong, C. K. Tse, and Q. Chen, "Analysis and comparison of secondary series- and parallel-compensated inductive power transfer systems operating for optimal efficiency and load-independent voltage-transfer ratio," *IEEE Trans. Power Electron.*, vol. 29, no. 6, pp. 2979–2990, Jun. 2014.

[17] S. Li and C. C. Mi, "Wireless power transfer for electric vehicle applications," *IEEE J. Emerg. Sel. Topics Power Electron.*, vol. 3, no. 1, pp. 4–17, Mar. 2015.

[18] A. Kurs, A. Karalis, R. Moffatt, J. D. Joannopoulos, P. Fisher, and M. Soljačić, "Wireless power transfer via strongly coupled magnetic resonances," *Science*, vol. 317, no. 5834, pp. 83–86, Jul. 2007.

[19] A. Kurs, R. Moffatt, and M. Soljačić, "Simultaneous mid-range power transfer to multiple devices," *Appl. Phys. Lett.*, vol. 96, no. 4, Jan. 2010, Art. no. 044102.

[20] A. P. Sample, D. T. Meyer, and J. R. Smith, "Analysis, experimental results, and range adaptation of magnetically coupled resonators for wireless power transfer," *IEEE Trans. Ind. Electron.*, vol. 58, no. 2, pp. 544–554, Feb. 2011.

[21] V. Vulfin, S. Sayfan-Altman, and R. Ianconescu, "Wireless power transfer for a pacemaker application," *J. Med. Eng. Technol.*, vol. 41, no. 4, pp. 325–332, May 2017.
[22] C. Xiao, D. Cheng, and K. Wei, "An LCC-C compensated wireless charging system for implantable cardiac pacemakers: Theory, experiment, and safety evaluation," *IEEE Trans. Power Electron.*, vol. 33, no. 6, pp. 4894–4905, Jun. 2018.
[23] C. Liu, C. Jiang, J. Song, and K. T. Chau, "An effective sandwiched wireless power transfer system for charging implantable cardiac pacemaker," *IEEE Trans. Ind. Electron.*, vol. 66, no. 5, pp. 4108–4117, May 2019.
[24] Md. R. Basar, M. Y. Ahmad, J. Cho, and F. Ibrahim, "Stable and high-efficiency wireless power transfer system for robotic capsule using a modified Helmholtz coil," *IEEE Trans. Ind. Electron.*, vol. 64, no. 2, pp. 1113–1122, Feb. 2017.
[25] H. Yigit and A. R. Boynuegri, "Pulsed laser diode based wireless power transmission application: Determination of voltage amplitude, frequency, and duty cycle," *IEEE Access*, vol. 11, pp. 54544–54555, 2023.
[26] A. Sagar, A. Kashyap, M. A. Nasab, S. Padmanaban, M. Bertoluzzo, A. Kumar, and F. Blaabjerg, "A comprehensive review of the recent development of wireless power transfer technologies for electric vehicle charging systems," *IEEE Access*, vol. 11, pp. 83703–83751, 2023.
[27] N. A. Khan, *Wireless Charger for Electric Vehicles With Electromagnetic Coil Based Position Correction*. Toronto, ON, Canada: Univ. Toronto, 2019.
[28] F. Corti, A. Reatti, M. C. Piccirilli, F. Grasso, L. Paolucci, and M. K. Kazimierczuk, "Simultaneous wireless power and data transfer: Overview and application to electric vehicles," in *Proc. IEEE Int. Symp. Circuits Syst. (ISCAS)*, Oct. 2020, pp. 1–5.
[29] C.-C. Huang, C.-L. Lin, and Y.-K. Wu, "Simultaneous wireless power/data transfer for electric vehicle charging," *IEEE Trans. Ind. Electron.*, vol. 64, no. 1, pp. 682–690, Jan. 2017.
[30] X. Chen-Yang, L. Chao-Wei, and Z. Juan, "Analysis of power transfer characteristic of capacitive power transfer system and inductively coupled power transfer system," in *Proc. Int. Conf. Mech. Sci., Electr. Eng. Comput. (MEC)*, Aug. 2011, pp. 1281–1285.
[31] D. van Wageningen and T. Staring, "The qi wireless power standard," in *Proc. 14th Int. Power Electron. Motion Control Conf. (EPE-PEMC)*, Sep. 2010, pp. S15–25.
[32] R. Tseng, B. von Novak, S. Shevde, and K. A. Grajski, "Introduction to the alliance for wireless power loosely-coupled wireless power transfer system specification version 1.0," in *Proc. IEEE Wireless Power Transf. (WPT)*, May 2013, pp. 79–83.
[33] S. D. Barman, A. W. Reza, N. Kumar, M. E. Karim, and A. B. Munir, "Wireless powering by magnetic resonant coupling: Recent trends in wireless power transfer system and its applications," *Renew. Sustain. Energy Rev.*, vol. 51, pp. 1525–1552, Nov. 2015.
[34] C. Liu, A. P. Hu, and N.-K.-C. Nair, "Modelling and analysis of a capacitively coupled contactless power transfer system," *IET Power Electron.*, vol. 4, no. 7, p. 808, 2011.
[35] C. Liu, A. P. Hu, and N.-K.-C. Nair, "Coupling study of a rotary capacitive power transfer system," in *Proc. IEEE Int. Conf. Ind. Technol.*, Feb. 2009, pp. 1–6.
[36] D. C. Ludois, J. K. Reed, and K. Hanson, "Capacitive power transfer for rotor field current in synchronous machines," *IEEE Trans. Power Electron.*, vol. 27, no. 11, pp. 4638–4645, Nov. 2012.
[37] M. Kline, I. Izyumin, B. Boser, and S. Sanders, "Capacitive power transfer for contactless charging," in *Proc. Twenty-Sixth Annu. IEEE Appl. Power Electron. Conf. Expo. (APEC)*, Mar. 2011, pp. 1398–1404.
[38] B. L. Cannon, J. F. Hoburg, D. D. Stancil, and S. C. Goldstein, "Magnetic resonant coupling as a potential means for wireless power transfer to multiple small receivers," *IEEE Trans. Power Electron.*, vol. 24, no. 7, pp. 1819–1825, Jul. 2009.
[39] N. A. Koondhar, M. Rehman, A. S. Saand, and M. Koondhar, "A Study of fundamental compensation topologies, performance parameters and designing a compensation for IPT for wireless charging applications," *J. Appl. Emerg. Sci.*, vol. 12, pp. 77–85, Dec. 2022.
[40] D. Kurschner, C. Rathge, and U. Jumar, "Design methodology for high efficient inductive power transfer systems with high coil positioning flexibility," *IEEE Trans. Ind. Electron.*, vol. 60, no. 1, pp. 372–381, Jan. 2013.
[41] T. Imura and Y. Hori, "Maximizing air gap and efficiency of magnetic resonant coupling for wireless power transfer using equivalent circuit and Neumann formula," *IEEE Trans. Ind. Electron.*, vol. 58, no. 10, pp. 4746–4752, Oct. 2011.
[42] S. L. Ho, J. Wang, W. N. Fu, and M. Sun, "A comparative study between novel witricity and traditional inductive magnetic coupling in wireless charging," *IEEE Trans. Magn.*, vol. 47, no. 5, pp. 1522–1525, May 2011.
[43] X. Wei, Z. Wang, and H. Dai, "A critical review of wireless power transfer via strongly coupled magnetic resonances," *Energies*, vol. 7, no. 7, pp. 4316–4341, Jul. 2014.
[44] S. Obayashi, Y. Kanekiyo, and T. Shijo, "UAV/drone fast wireless charging FRP frustum port for 85-kHz 50-V 10-A inductive power transfer," in *Proc. IEEE Wireless Power Transf. Conf. (WPTC)*, Nov. 2020, pp. 219–222.
[45] T.-S. Lee, S.-J. Huang, and M.-J. Wu, "Enhancement of wireless power transfer for automated guided vehicles considering disturbance suppression," *IEEE Access*, vol. 11, pp. 21508–21518, 2023.
[46] H. Wang and K. W. E. Cheng, "A dual-receiver inductive charging system for automated guided vehicles," *IEEE Trans. Magn.*, vol. 58, no. 8, pp. 1–5, Aug. 2022.
[47] A. A. S. Mohamed and O. Mohammed, "Physics-based co-simulation platform with analytical and experimental verification for bidirectional IPT system in EV applications," *IEEE Trans. Veh. Technol.*, vol. 67, no. 1, pp. 275–284, Jan. 2018.
[48] S. Weerasinghe, D. J. Thrimawithana, and U. K. Madawala, "Modeling bidirectional contactless grid interfaces with a soft DC-link," *IEEE Trans. Power Electron.*, vol. 30, no. 7, pp. 3528–3541, Jul. 2015.
[49] H. Zeng, S. Yang, and F. Z. Peng, "Design consideration and comparison of wireless power transfer via harmonic current for PHEV and EV wireless charging," *IEEE Trans. Power Electron.*, vol. 32, no. 8, pp. 5943–5952, Aug. 2017.
[50] L. Wang, U. K. Madawala, and M.-C. Wong, "A wireless vehicle-to-grid-to-home power interface with an adaptive DC link," *IEEE J. Emerg. Sel. Topics Power Electron.*, vol. 9, no. 2, pp. 2373–2383, Apr. 2021.
[51] H. Z. Z. Beh, G. A. Covic, and J. T. Boys, "Investigation of magnetic couplers in bicycle kickstands for wireless charging of electric bicycles," *IEEE J. Emerg. Sel. Topics Power Electron.*, vol. 3, no. 1, pp. 87–100, Mar. 2015.
[52] A. Hossain, P. Darvish, S. Mekhilef, K. S. Tey, and C. W. Tong, "A new coil structure of dual transmitters and dual receivers with integrated decoupling coils for increasing power transfer and misalignment tolerance of wireless EV charging system," *IEEE Trans. Ind. Electron.*, vol. 69, no. 8, pp. 7869–7878, Aug. 2022.
[53] H. Wang, K. W. E. Cheng, and Y. Yang, "A new resonator design for wireless battery charging systems of electric bicycles," *IEEE J. Emerg. Sel. Topics Power Electron.*, vol. 10, no. 5, pp. 6009–6019, Oct. 2022.
[54] S. A. A. Shah and H. Yoo, "Radiative near-field wireless power transfer to scalp-implantable biotelemetric device," *IEEE Trans. Microw. Theory Techn.*, vol. 68, no. 7, pp. 2944–2953, Jul. 2020.
[55] P. Meyer, *Modeling of Inductive Contactless Energy Transfer Systems*. Lausanne, Switzerland: EPFL, 2012.
[56] Y. H. Sohn, B. H. Choi, E. S. Lee, G. C. Lim, G.-H. Cho, and C. T. Rim, "General unified analyses of two-capacitor inductive power transfer systems: Equivalence of current-source SS and SP compensations," *IEEE Trans. Power Electron.*, vol. 30, no. 11, pp. 6030–6045, Nov. 2015.
[57] W. Zhong, C. K. Lee, and S. Y. R. Hui, "General analysis on the use of Tesla's resonators in domino forms for wireless power transfer," *IEEE Trans. Ind. Electron.*, vol. 60, no. 1, pp. 261–270, Jan. 2013.
[58] Y. Wang, Y. Yao, X. Liu, and D. Xu, "S/CLC compensation topology analysis and circular coil design for wireless power transfer," *IEEE Trans. Transport. Electrific.*, vol. 3, no. 2, pp. 496–507, Jun. 2017.
[59] X. Zhang, S. L. Ho, and W. N. Fu, "Quantitative design and analysis of relay resonators in wireless power transfer system," *IEEE Trans. Magn.*, vol. 48, no. 11, pp. 4026–4029, Nov. 2012.
[60] W. X. Zhong, C. K. Lee, and S. Y. Hui, "Wireless power domino-resonator systems with noncoaxial axes and circular structures," *IEEE Trans. Power Electron.*, vol. 27, no. 11, pp. 4750–4762, Nov. 2012.
[61] C. K. Lee, W. X. Zhong, and S. Y. R. Hui, "Effects of magnetic coupling of nonadjacent resonators on wireless power domino-resonator systems," *IEEE Trans. Power Electron.*, vol. 27, no. 4, pp. 1905–1916, Apr. 2012.
[62] M. Rayes, G. Nagib, and W. Abdelaal, "A review on wireless power transfer," *Int. J. Eng. Trends Technol.*, vol. 40, no. 5, pp. 272–280, Oct. 2016.
[63] H. H. Wu, A. Gilchrist, K. D. Sealy, and D. Bronson, "A high efficiency 5 kW inductive charger for EVs using dual side control," *IEEE Trans. Ind. Informat.*, vol. 8, no. 3, pp. 585–595, Aug. 2012.

[64] S. Jeong, Y. J. Jang, and D. Kum, "Economic analysis of the dynamic charging electric vehicle," *IEEE Trans. Power Electron.*, vol. 30, no. 11, pp. 6368–6377, Nov. 2015.

[65] S. Aldhaher, P. C. Luk, and J. F. Whidborne, "Electronic tuning of misaligned coils in wireless power transfer systems," *IEEE Trans. Power Electron.*, vol. 29, no. 11, pp. 5975–5982, Nov. 2014.

[66] M. Budhia, G. A. Covic, J. T. Boys, and C.-Y. Huang, "Development and evaluation of single sided flux couplers for contactless electric vehicle charging," in *Proc. IEEE Energy Convers. Congr. Expo.*, Sep. 2011, pp. 614–621.

[67] Q. Zhu, L. Wang, Y. Guo, C. Liao, and F. Li, "Applying LCC compensation network to dynamic wireless EV charging system," *IEEE Trans. Ind. Electron.*, vol. 63, no. 10, pp. 6557–6567, Oct. 2016.

[68] B. Schmuelling, S. G. Cimen, T. Vosshagen, and F. Turki, "Layout and operation of a non-contact charging system for electric vehicles," in *Proc. 15th Int. Power Electron. Motion Control Conf. (EPE/PEMC)*, Sep. 2012, pp. LS4d.4-1–LS4d.4-7.

[69] J. L. Villa, A. Llombart, J. F. Sanz, and J. Sallan, "Practical development of a 5 kW ICPT system SS compensated with a large air gap," in *Proc. IEEE Int. Symp. Ind. Electron.*, Jun. 2007, pp. 1219–1223.

[70] R. Laouamer, M. Brunello, J. P. Ferrieux, O. Normand, and N. Buchheit, "A multi-resonant converter for non-contact charging with electromagnetic coupling," in *Proc. IECON 23rd Int. Conf. Ind. Electron., Control, Instrum.*, Nov. 1997, pp. 792–797.

[71] M. Budhia, G. Covic, and J. Boys, "A new IPT magnetic coupler for electric vehicle charging systems," in *Proc. IECON 36th Annu. Conf. IEEE Ind. Electron. Soc.*, Nov. 2010, pp. 2487–2492.

[72] G. A. Covic, M. L. G. Kissin, D. Kacprzak, N. Clausen, and H. Hao, "A bipolar primary pad topology for EV stationary charging and highway power by inductive coupling," in *Proc. IEEE Energy Convers. Congr. Expo.*, Sep. 2011, pp. 1832–1838.

[73] S. Raabe, G. A. J. Elliott, G. A. Covic, and J. T. Boys, "A quadrature pickup for inductive power transfer systems," in *Proc. 2nd IEEE Conf. Ind. Electron. Appl.*, May 2007, pp. 68–73.

[74] M. L. G. Kissin, G. A. Covic, and J. T. Boys, "Estimating the output power of flat pickups in complex IPT systems," in *Proc. IEEE Power Electron. Spec. Conf.*, Jun. 2008, pp. 604–610.

[75] M. L. G. Kissin, J. T. Boys, and G. A. Covic, "Interphase mutual inductance in polyphase inductive power transfer systems," *IEEE Trans. Ind. Electron.*, vol. 56, no. 7, pp. 2393–2400, Jul. 2009.

[76] Y. Shanmugam, N. R, P. Vishnuram, M. Bajaj, K. M. AboRas, P. Thakur, and Kitmo, "A systematic review of dynamic wireless charging system for electric transportation," *IEEE Access*, vol. 10, pp. 133617–133642, 2022.

[77] M.-H. Park, E.-G. Shin, H.-R. Lee, and I.-S. Suh, "Dynamic model and control algorithm of HVAC system for OLEV application," in *Proc. ICCAS*, Oct. 2010, pp. 1312–1317.

[78] J. Shin, B. Song, S. Lee, S. Shin, Y. Kim, G. Jung, and S. Jeon, "Contactless power transfer systems for on-line electric vehicle (OLEV)," in *Proc. IEEE Int. Electr. Vehicle Conf.*, Mar. 2012, pp. 1–4.

[79] B. Song, J. Shin, S. Chung, S. Shin, S. Lee, Y. Kim, G. Jung, and S. Jeon, "Design of a pickup with compensation winding for on-line electric vehicle (OLEV)," in *Proc. IEEE Wireless Power Transf. (WPT)*, May 2013, pp. 60–62.

[80] B. Song, J. Shin, S. Lee, S. Shin, Y. Kim, S. Jeon, and G. Jung, "Design of a high power transfer pickup for on-line electric vehicle (OLEV)," in *Proc. IEEE Int. Electr. Vehicle Conf.*, Mar. 2012, pp. 1–4.

[81] J. L. Villa, J. Sallán, A. Llombart, and J. F. Sanz, "Design of a high frequency inductively coupled power transfer system for electric vehicle battery charge," *Appl. Energy*, vol. 86, no. 3, pp. 355–363, Mar. 2009.

[82] J. Zhang, X. Yuan, C. Wang, and Y. He, "Comparative analysis of two-coil and three-coil structures for wireless power transfer," *IEEE Trans. Power Electron.*, vol. 32, no. 1, pp. 341–352, Jan. 2017.

[83] L. Chen, S. Liu, Y. C. Zhou, and T. J. Cui, "An optimizable circuit structure for high-efficiency wireless power transfer," *IEEE Trans. Ind. Electron.*, vol. 60, no. 1, pp. 339–349, Jan. 2013.

[84] P. Vishnuram, S. Panchanathan, N. Rajamanickam, V. Krishnasamy, M. Bajaj, M. Piecha, V. Blazek, and L. Prokop, "Review of wireless charging system: Magnetic materials, coil configurations, challenges, and future perspectives," *Energies*, vol. 16, no. 10, p. 4020, May 2023.

[85] A. J. Moradewicz and M. P. Kazmierkowski, "Contactless energy transfer system with FPGA-controlled resonant converter," *IEEE Trans. Ind. Electron.*, vol. 57, no. 9, pp. 3181–3190, Sep. 2010.

[86] J. Rahulkumar., R. Narayanamoorthi, P. Vishnuram, M. Bajaj, V. Blazek, L. Prokop, and S. Misak, "An empirical survey on wireless inductive power pad and resonant magnetic field coupling for in-motion EV charging system," *IEEE Access*, vol. 11, pp. 4660–4693, 2023.

[87] J. G. Bolger, F. A. Kirsten, and L. S. Ng, "Inductive power coupling for an electric highway system," in *Proc. 28th IEEE Veh. Technol. Conf.*, Mar. 1978, pp. 137–144.

[88] C.-S. Wang, O. H. Stielau, and G. A. Covic, "Design considerations for a contactless electric vehicle battery charger," *IEEE Trans. Ind. Electron.*, vol. 52, no. 5, pp. 1308–1314, Oct. 2005.

[89] J. M. Miller, C. P. White, O. C. Onar, and P. M. Ryan, "Grid side regulation of wireless power charging of plug-in electric vehicles," in *Proc. IEEE Energy Convers. Congr. Expo. (ECCE)*, Sep. 2012, pp. 261–268.

[90] J. Kim, J. Kim, S. Kong, H. Kim, I.-S. Suh, N. P. Suh, D.-H. Cho, J. Kim, and S. Ahn, "Coil design and shielding methods for a magnetic resonant wireless power transfer system," *Proc. IEEE*, vol. 101, no. 6, pp. 1332–1342, Jun. 2013.

[91] Y. Nagatsuka, N. Ehara, Y. Kaneko, S. Abe, and T. Yasuda, "Compact contactless power transfer system for electric vehicles," in *Proc. Int. Power Electron. Conf. (ECCE ASIA)*, Jun. 2010, pp. 807–813.

[92] R. Bosshard, J. W. Kolar, J. Mühlethaler, I. Stevanović, B. Wunsch, and F. Canales, "Modeling and η-α-Pareto optimization of inductive power transfer coils for electric vehicles," *IEEE J. Emerg. Sel. Topics Power Electron.*, vol. 3, no. 1, pp. 50–64, Mar. 2015.

[93] R. Bosshard and J. W. Kolar, "Multi-objective optimization of 50 kW/85 kHz IPT system for public transport," *IEEE J. Emerg. Sel. Topics Power Electron.*, vol. 4, no. 4, pp. 1370–1382, Dec. 2016.

[94] Y. Lim, H. Tang, S. Lim, and J. Park, "An adaptive impedance-matching network based on a novel capacitor matrix for wireless power transfer," *IEEE Trans. Power Electron.*, vol. 29, no. 8, pp. 4403–4413, Aug. 2014.

[95] A. Kamineni, G. A. Covic, and J. T. Boys, "Analysis of coplanar intermediate coil structures in inductive power transfer systems," *IEEE Trans. Power Electron.*, vol. 30, no. 11, pp. 6141–6154, Nov. 2015.

[96] B. H. Choi, E. S. Lee, J. Huh, and C. T. Rim, "Lumped impedance transformers for compact and robust coupled magnetic resonance systems," *IEEE Trans. Power Electron.*, vol. 30, no. 11, pp. 6046–6056, Nov. 2015.

[97] D. Ahn and S. Hong, "A study on magnetic field repeater in wireless power transfer," *IEEE Trans. Ind. Electron.*, vol. 60, no. 1, pp. 360–371, Jan. 2013.

[98] A. Zakerian, S. Vaez-Zadeh, and A. Babaki, "A dynamic WPT system with high efficiency and high power factor for electric vehicles," *IEEE Trans. Power Electron.*, vol. 35, no. 7, pp. 6732–6740, Jul. 2020.

[99] L. Yang, X. Li, S. Liu, Z. Xu, C. Cai, and P. Guo, "Analysis and design of three-coil structure WPT system with constant output current and voltage for battery charging applications," *IEEE Access*, vol. 7, pp. 87334–87344, 2019.

[100] Y. Li, J. Hu, M. Liu, Y. Chen, K. W. Chan, Z. He, and R. Mai, "Reconfigurable intermediate resonant circuit based WPT system with load-independent constant output current and voltage for charging battery," *IEEE Trans. Power Electron.*, vol. 34, no. 3, pp. 1988–1992, Mar. 2019.

[101] W. Li, H. Zhao, S. Li, J. Deng, T. Kan, and C. C. Mi, "Integrated *LCC* compensation topology for wireless charger in electric and plug-in electric vehicles," *IEEE Trans. Ind. Electron.*, vol. 62, no. 7, pp. 4215–4225, Jul. 2015.

[102] J. Deng, W. Li, T. D. Nguyen, S. Li, and C. C. Mi, "Compact and efficient bipolar coupler for wireless power chargers: Design and analysis," *IEEE Trans. Power Electron.*, vol. 30, no. 11, pp. 6130–6140, Nov. 2015.

[103] S. Li, W. Li, J. Deng, T. D. Nguyen, and C. C. Mi, "A double-sided LCC compensation network and its tuning method for wireless power transfer," *IEEE Trans. Veh. Technol.*, vol. 64, no. 6, pp. 2261–2273, Jun. 2015.

[104] F. Lu, H. Zhang, H. Hofmann, and C. C. Mi, "An inductive and capacitive combined wireless power transfer system with LC-compensated topology," *IEEE Trans. Power Electron.*, vol. 31, no. 12, pp. 8471–8482, Dec. 2016.

[105] T. C. Beh, M. Kato, T. Imura, S. Oh, and Y. Hori, "Automated impedance matching system for robust wireless power transfer via magnetic resonance coupling," *IEEE Trans. Ind. Electron.*, vol. 60, no. 9, pp. 3689–3698, Sep. 2013.

[106] J. Bito, S. Jeong, and M. M. Tentzeris, "A novel heuristic passive and active matching circuit design method for wireless power transfer to moving objects," *IEEE Trans. Microw. Theory Techn.*, vol. 65, no. 4, pp. 1094–1102, Apr. 2017.

[107] B. H. Waters, A. P. Sample, and J. Smith, "Adaptive impedance matching for magnetically coupled resonators," *Prog. Electromagn. Res.*, pp. 694–701, 2012.
[108] D.-W. Seo, J.-H. Lee, and H. Lee, "A study on two-coil and four-coil wireless power transfer system using Z-parameter approach," *ETRI J.*, vol. 38, pp. 568–578, Feb. 2016.
[109] J. C. McLaughlin and K. Kaiser, "Deglorifying' the maximum power transfer theorem and factors in impedance selection," *IEEE Trans. Educ.*, vol. 50, no. 3, pp. 251–255, Aug. 2007.
[110] J. Bito, S. Jeong, and M. M. Tentzeris, "A real-time electrically controlled active matching circuit utilizing genetic algorithms for wireless power transfer to biomedical implants," *IEEE Trans. Microw. Theory Techn.*, vol. 64, no. 2, pp. 365–374, Feb. 2016.
[111] Z. Miao, D. Liu, and C. Gong, "An adaptive impedance matching network with closed loop control algorithm for inductive wireless power transfer," *Sensors*, vol. 17, no. 8, p. 1759, Aug. 2017.
[112] S. Liu, L. Chen, Y. Zhou, and T. J. Cui, "A general theory to analyse and design wireless power transfer based on impedance matching," *Int. J. Electron.*, vol. 101, no. 10, pp. 1375–1404, Oct. 2014.
[113] B. Esteban, M. Sid-Ahmed, and N. C. Kar, "A comparative study of power supply architectures in wireless EV charging systems," *IEEE Trans. Power Electron.*, vol. 30, no. 11, pp. 6408–6422, Nov. 2015.
[114] M. Rozman, M. Fernando, B. Adebisi, K. Rabie, T. Collins, R. Kharel, and A. Ikpehai, "A new technique for reducing size of a WPT system using two-loop strongly-resonant inductors," *Energies*, vol. 10, no. 10, p. 1614, Oct. 2017.
[115] X.-Y. Yan, S.-C. Yang, H. He, and T.-Q. Tang, "An optimization model for wireless power transfer system based on circuit simulation," *Phys. A, Stat. Mech. Appl.*, vol. 509, pp. 873–880, Nov. 2018.
[116] Y. Wang, Y. Yao, X. Liu, D. Xu, and L. Cai, "An LC/S compensation topology and coil design technique for wireless power transfer," *IEEE Trans. Power Electron.*, vol. 33, no. 3, pp. 2007–2025, Mar. 2018.
[117] A. Ong, J. P. K. Sampath, G. F. H. Beng, T. YenKheng, D. M. Vilathgamuwa, and N. X. Bac, "Analysis of impedance matched circuit for wireless power transfer," in *Proc. IECON 40th Annu. Conf. IEEE Ind. Electron. Soc.*, Oct. 2014, pp. 2965–2970.
[118] H. Nguyen and J. I. Agbinya, "Splitting frequency diversity in wireless power transmission," *IEEE Trans. Power Electron.*, vol. 30, no. 11, pp. 6088–6096, Nov. 2015.
[119] N. T. Diep, N. K. Trung, and T. T. Minh, "Design and analysis of coupling system in electric vehicle dynamic wireless charging applications," in *Proc. IEEE Vehicle Power Propuls. Conf. (VPPC)*, Oct. 2019, pp. 1–6.
[120] S. Khan and G. Choi, "Analysis and optimization of four-coil planar magnetically coupled printed spiral resonators," *Sensors*, vol. 16, no. 8, p. 1219, Aug. 2016.
[121] Y. Li, Q. Xu, T. Lin, J. Hu, Z. He, and R. Mai, "Analysis and design of load-independent output current or output voltage of a three-coil wireless power transfer system," *IEEE Trans. Transport. Electrific.*, vol. 4, no. 2, pp. 364–375, Jun. 2018.
[122] D. De Marco, A. Dolara, M. Longo, and W. Yaïci, "Design and performance analysis of pads for dynamic wireless charging of EVs using the finite element method," *Energies*, vol. 12, no. 21, p. 4139, Oct. 2019.
[123] L. Strauch, M. Pavlin, and V. B. Bregar, "Optimization, design, and modeling of ferrite core geometry for inductive wireless power transfer," *Int. J. Appl. Electromagn. Mech.*, vol. 49, no. 1, pp. 145–155, Sep. 2015.
[124] M. Alam, S. Mekhilef, M. Seyedmahmoudian, and B. Horan, "Dynamic charging of electric vehicle with negligible power transfer fluctuation," *Energies*, vol. 10, no. 5, p. 701, May 2017.
[125] K. Fotopoulou and B. W. Flynn, "Wireless power transfer in loosely coupled links: Coil misalignment model," *IEEE Trans. Magn.*, vol. 47, no. 2, pp. 416–430, Feb. 2011.
[126] J. Rahulkumar, R. Narayanamoorthi, P. Vishnuram, C. Balaji, T. Gono, T. Dockal, R. Gono, and P. Krejci, "A review on resonant inductive coupling pad design for wireless electric vehicle charging application," *Energy Rep.*, vol. 10, pp. 2047–2079, Nov. 2023.
[127] X. Qu, H. Han, S.-C. Wong, C. K. Tse, and W. Chen, "Hybrid IPT topologies with constant current or constant voltage output for battery charging applications," *IEEE Trans. Power Electron.*, vol. 30, no. 11, pp. 6329–6337, Nov. 2015.
[128] M. Rehman, Z. Baharudin, P. Nallagownden, and B. Ul Islam, "Modelling and efficiency-analysis of wireless power transfer using magnetic resonance coupling," *Indonesian J. Electr. Eng. Comput. Sci.*, vol. 6, no. 3, p. 563, Jun. 2017.
[129] M. Rehman, Z. Baharudin, P. Nallagownden, B. Islam, and M. J. I. Rehman, "Modeling and analysis of series-series and series-parallel combined topology for wireless power transfer using multiple coupling coefficients," *IJCSNS*, vol. 17, p. 114, Nov. 2017.
[130] T. Linlin, Q. Hao, H. Xueliang, C. Weijie, and S. Wenhui, "A novel optimization means of transfer efficiency for resonance coupled wireless power transfer," *TELKOMNIKA Indonesian J. Electr. Eng.*, vol. 11, no. 5, pp. 2747–2752, May 2013.
[131] L. J. Yu, "Finite element analysis of a contactless power transformer with metamaterial," *TELKOMNIKA Indonesian J. Electr. Eng.*, vol. 12, no. 1, pp. 678–684, Jan. 2014.
[132] D. Zhao, E. Ding, Y. Hu, and Z. Sun, "Design and simulation of multiple coil model for wireless power transmission system," *TELKOMNIKA Indonesian J. Electr. Eng.*, vol. 12, no. 6, pp. 4166–4177, Jun. 2014.
[133] C. Yahaya, S. F. S. Adnan, M. Kassim, R. A. Rahman, and M. F. B. Rusdi, "Analysis of wireless power transfer on the inductive coupling resonant," *Indones. J. Electr. Eng. Comput. Sci.*, vol. 12, no. 2, pp. 592–599, 2018.
[134] M. Alam, S. Mekhilef, H. Bassi, and M. Rawa, "Analysis of LC-LC_2 compensated inductive power transfer for high efficiency and load independent voltage gain," *Energies*, vol. 11, no. 11, p. 2883, Oct. 2018.
[135] J. Kim, D.-H. Kim, and Y.-J. Park, "Analysis of capacitive impedance matching networks for simultaneous wireless power transfer to multiple devices," *IEEE Trans. Ind. Electron.*, vol. 62, no. 5, pp. 2807–2813, May 2015.
[136] W. Zhang, S.-C. Wong, C. K. Tse, and Q. Chen, "Design for efficiency optimization and voltage controllability of series–series compensated inductive power transfer systems," *IEEE Trans. Power Electron.*, vol. 29, no. 1, pp. 191–200, Jan. 2014.
[137] J. Shin, S. Shin, Y. Kim, S. Ahn, S. Lee, G. Jung, S.-J. Jeon, and D.-H. Cho, "Design and implementation of shaped magnetic-resonance-based wireless power transfer system for roadway-powered moving electric vehicles," *IEEE Trans. Ind. Electron.*, vol. 61, no. 3, pp. 1179–1192, Mar. 2014.
[138] Q. Chen, S. C. Wong, C. K. Tse, and X. Ruan, "Analysis, design, and control of a transcutaneous power regulator for artificial hearts," *IEEE Trans. Biomed. Circuits Syst.*, vol. 3, no. 1, pp. 23–31, Feb. 2009.
[139] X. Ren, Q. Chen, L. Cao, X. Ruan, S.-C. Wong, and Chi. K. Tse, "Characterization and control of self-oscillating contactless resonant converter with fixed voltage gain," in *Proc. 7th Int. Power Electron. Motion Control Conf.*, vol. 3, Jun. 2012, pp. 1822–1827.
[140] K. Kusaka, K. Inoue, and J.-I. Itoh, "Inductive power transfer system for an excavator by considering large load fluctuation," *IEEJ J. Ind. Appl.*, vol. 8, no. 3, pp. 413–420, 2019.
[141] S. Hasanzadeh and S. Vaez-Zadeh, "Enhancement of overall coupling coefficient and efficiency of contactless energy transmission systems," in *Proc. 2nd Power Electron., Drive Syst. Technol. Conf.*, Feb. 2011, pp. 638–643.
[142] J. Hou, Q. Chen, S.-C. Wong, C. K. Tse, and X. Ruan, "Analysis and control of series/series-parallel compensated resonant converter for contactless power transfer," *IEEE J. Emerg. Sel. Topics Power Electron.*, vol. 3, no. 1, pp. 124–136, Mar. 2015.
[143] I. Nam, R. Dougal, and E. Santi, "Optimal design method to achieve both good robustness and efficiency in loosely-coupled wireless charging system employing series-parallel resonant tank with asymmetrical magnetic coupler," in *Proc. IEEE Energy Convers. Congr. Expo.*, Sep. 2013, pp. 3266–3276.
[144] C.-S. Wang, G. A. Covic, and O. H. Stielau, "Power transfer capability and bifurcation phenomena of loosely coupled inductive power transfer systems," *IEEE Trans. Ind. Electron.*, vol. 51, no. 1, pp. 148–157, Feb. 2004.
[145] E. R. Joy, B. K. Kushwaha, G. Rituraj, and P. Kumar, "Analysis and comparison of four compensation topologies of contactless power transfer system," in *Proc. 4th Int. Conf. Electr. Power Energy Convers. Syst. (EPECS)*, Nov. 2015, pp. 1–6.
[146] J. L. Villa, J. Sallan, J. F. Sanz Osorio, and A. Llombart, "High-misalignment tolerant compensation topology for ICPT systems," *IEEE Trans. Ind. Electron.*, vol. 59, no. 2, pp. 945–951, Feb. 2012.
[147] J. Hou, Q. Chen, K. Yan, X. Ren, S.-C. Wong, and Chi. K. Tse, "Analysis and control of S/SP compensation contactless resonant converter with constant voltage gain," in *Proc. IEEE Energy Convers. Congr. Expo.*, Sep. 2013, pp. 2552–2558.

[148] X. Liu, L. Clare, X. Yuan, C. Wang, and J. Liu, "A design method for making an LCC compensation two-coil wireless power transfer system more energy efficient than an SS counterpart," *Energies*, vol. 10, no. 9, p. 1346, Sep. 2017.

[149] F. Lu, H. Zhang, H. Hofmann, and C. C. Mi, "A dynamic charging system with reduced output power pulsation for electric vehicles," *IEEE Trans. Ind. Electron.*, vol. 63, no. 10, pp. 6580–6590, Oct. 2016.

[150] Y. Chen, H. Zhang, C.-S. Shin, K.-H. Seo, S.-J. Park, and D.-H. Kim, "A comparative study of S-S and LCC-S compensation topology of inductive power transfer systems for EV chargers," in *Proc. IEEE 10th Int. Symp. Power Electron. Distrib. Gener. Syst. (PEDG)*, Jun. 2019, pp. 99–104.

[151] A. Ramezani, S. Farhangi, H. Iman-Eini, B. Farhangi, R. Rahimi, and G. R. Moradi, "Optimized LCC-series compensated resonant network for stationary wireless EV chargers," *IEEE Trans. Ind. Electron.*, vol. 66, no. 4, pp. 2756–2765, Apr. 2019.

[152] Z. Yan, Y. Zhang, B. Song, K. Zhang, T. Kan, and C. Mi, "An LCC-P compensated wireless power transfer system with a constant current output and reduced receiver size," *Energies*, vol. 12, no. 1, p. 172, Jan. 2019.

[153] C.-Y. Huang, J. T. Boys, and G. A. Covic, "LCL pickup circulating current controller for inductive power transfer systems," *IEEE Trans. Power Electron.*, vol. 28, no. 4, pp. 2081–2093, Apr. 2013.

[154] N. A. Keeling, G. A. Covic, and J. T. Boys, "A unity-power-factor IPT pickup for high-power applications," *IEEE Trans. Ind. Electron.*, vol. 57, no. 2, pp. 744–751, Feb. 2010.

[155] S. Raabe and G. A. Covic, "Practical design considerations for contactless power transfer quadrature pick-ups," *IEEE Trans. Ind. Electron.*, vol. 60, no. 1, pp. 400–409, Jan. 2013.

[156] M. Amjad, Z. Salam, M. Facta, and S. Mekhilef, "Analysis and implementation of transformerless LCL resonant power supply for ozone generation," *IEEE Trans. Power Electron.*, vol. 28, no. 2, pp. 650–660, Feb. 2013.

[157] Y. Yao, Y. Wang, X. Liu, F. Lin, and D. Xu, "A novel parameter tuning method for a double-sided LCL compensated WPT system with better comprehensive performance," *IEEE Trans. Power Electron.*, vol. 33, no. 10, pp. 8525–8536, Oct. 2018.

[158] M. Venkatesan, N. Rajamanickam, P. Vishnuram, M. Bajaj, V. Blazek, L. Prokop, and S. Misak, "A review of compensation topologies and control techniques of bidirectional wireless power transfer systems for electric vehicle applications," *Energies*, vol. 15, no. 20, p. 7816, Oct. 2022.

[159] A. Yu, X. Zeng, D. Xiong, M. Tian, and J. Li, "An improved autonomous current-fed push-pull parallel-resonant inverter for inductive power transfer system," *Energies*, vol. 11, no. 10, p. 2653, Oct. 2018.

[160] L. Gallucci, C. Menna, L. Angrisani, D. Asprone, R. S. L. Moriello, F. Bonavolontà, and F. Fabbrocino, "An embedded wireless sensor network with wireless power transmission capability for the structural health monitoring of reinforced concrete structures," *Sensors*, vol. 17, no. 11, p. 2566, Nov. 2017.

[161] D. Ahn and S. Hong, "Wireless power transmission with self-regulated output voltage for biomedical implant," *IEEE Trans. Ind. Electron.*, vol. 61, no. 5, pp. 2225–2235, May 2014.

[162] S. Samanta and A. K. Rathore, "Analysis and design of load-independent ZPA operation for P/S, PS/S, P/SP, and PS/SP tank networks in IPT applications," *IEEE Trans. Power Electron.*, vol. 33, no. 8, pp. 6476–6482, Aug. 2018.

[163] Z. Ning Low, R. A. Chinga, R. Tseng, and J. Lin, "Design and test of a high-power high-efficiency loosely coupled planar wireless power transfer system," *IEEE Trans. Ind. Electron.*, vol. 56, no. 5, pp. 1801–1812, May 2009.

[164] I. U. Castillo-Zamora, P. S. Huynh, D. Vincent, F. J. Perez-Pinal, M. A. Rodriguez-Licea, and S. S. Williamson, "Hexagonal geometry coil for a WPT high-power fast charging application," *IEEE Trans. Transport. Electrific.*, vol. 5, no. 4, pp. 946–956, Dec. 2019.

[165] M. G. Kim, Y. R. Lee, and J. R. Choi, "Wireless power transmission of a smartphone by three-dimensional magnetic resonance," in *Proc. 16th Int. Conf. Synth., Modeling, Anal. Simulation Methods Appl. Circuit Design (SMACD)*, Jul. 2019, pp. 117–120.

[166] R. Venugopal, C. Balaji, A. Dominic Savio, R. Narayanamoorthi, K. M. AboRas, H. Kotb, Y. Y. Ghadi, M. Shouran, and E. Elgamli, "Review on unidirectional non-isolated high gain DC–DC converters for EV sustainable DC fast charging applications," *IEEE Access*, vol. 11, pp. 78299–78338, May 2023.

[167] X. Zhang, Z. Yuan, Q. Yang, Y. Li, J. Zhu, and Y. Li, "Coil design and efficiency analysis for dynamic wireless charging system for electric vehicles," *IEEE Trans. Magn.*, vol. 52, no. 7, pp. 1–4, Jul. 2016.

[168] V. Prasanth and P. Bauer, "Study of misalignment for on road charging," in *Proc. IEEE Transp. Electrific. Conf. Expo. (ITEC)*, Jun. 2013, pp. 1–8.

[169] W. Zhang, S.-C. Wong, C. K. Tse, and Q. Chen, "An optimized track length in roadway inductive power transfer systems," *IEEE J. Emerg. Sel. Topics Power Electron.*, vol. 2, no. 3, pp. 598–608, Sep. 2014.

[170] F. F. A. van der Pijl, M. Castilla, and P. Bauer, "Adaptive sliding-mode control for a multiple-user inductive power transfer system without need for communication," *IEEE Trans. Ind. Electron.*, vol. 60, no. 1, pp. 271–279, Jan. 2013.

[171] O. C. Onar, J. M. Miller, S. L. Campbell, C. Coomer, Cliff. P. White, and L. E. Seiber, "A novel wireless power transfer for in-motion EV/PHEV charging," in *Proc. 28th Annu. IEEE Appl. Power Electron. Conf. Expo. (APEC)*, Mar. 2013, pp. 3073–3080.

[172] J. M. Miller, P. T. Jones, J.-M. Li, and O. C. Onar, "ORNL experience and challenges facing dynamic wireless power charging of EV's," *IEEE Circuits Syst. Mag.*, vol. 15, no. 2, pp. 40–53, 2nd Quart., 2015.

[173] H. Li, K. Wang, L. Huang, J. Li, and X. Yang, "Coil structure optimization method for improving coupling coefficient of wireless power transfer," in *Proc. IEEE Appl. Power Electron. Conf. Expo. (APEC)*, Mar. 2015, pp. 2518–2521.

[174] G. A. Covic, J. T. Boys, M. L. G. Kissin, and H. G. Lu, "A three-phase inductive power transfer system for roadway-powered vehicles," *IEEE Trans. Ind. Electron.*, vol. 54, no. 6, pp. 3370–3378, Dec. 2007.

[175] Y. D. Ko and Y. J. Jang, "The optimal system design of the online electric vehicle utilizing wireless power transmission technology," *IEEE Trans. Intell. Transp. Syst.*, vol. 14, no. 3, pp. 1255–1265, Sep. 2013.

[176] W. Y. Lee, J. Huh, S. Y. Choi, X. V. Thai, J. H. Kim, E. A. Al-Ammar, M. A. El-Kady, and C. T. Rim, "Finite-width magnetic mirror models of mono and dual coils for wireless electric vehicles," *IEEE Trans. Power Electron.*, vol. 28, no. 3, pp. 1413–1428, Mar. 2013.

[177] S. Choi, J. Huh, W. Y. Lee, S. W. Lee, and C. T. Rim, "New cross-segmented power supply rails for roadway-powered electric vehicles," *IEEE Trans. Power Electron.*, vol. 28, no. 12, pp. 5832–5841, Dec. 2013.

[178] S. Y. Choi, B. W. Gu, S. W. Lee, W. Y. Lee, J. Huh, and C. T. Rim, "Generalized active EMF cancel methods for wireless electric vehicles," *IEEE Trans. Power Electron.*, vol. 29, no. 11, pp. 5770–5783, Nov. 2014.

[179] J. Huh, S. W. Lee, W. Y. Lee, G. H. Cho, and C. T. Rim, "Narrow-width inductive power transfer system for online electrical vehicles," *IEEE Trans. Power Electron.*, vol. 26, no. 12, pp. 3666–3679, Dec. 2011.

[180] G. Elliott, S. Raabe, G. A. Covic, and J. T. Boys, "Multiphase pickups for large lateral tolerance contactless power-transfer systems," *IEEE Trans. Ind. Electron.*, vol. 57, no. 5, pp. 1590–1598, May 2010.

[181] K. Lee, Z. Pantic, and S. M. Lukic, "Reflexive field containment in dynamic inductive power transfer systems," *IEEE Trans. Power Electron.*, vol. 29, no. 9, pp. 4592–4602, Sep. 2014.

[182] T.-D. Nguyen, S. Li, W. Li, and C. C. Mi, "Feasibility study on bipolar pads for efficient wireless power chargers," in *Proc. IEEE Appl. Power Electron. Conf. Expo. (APEC)*, Mar. 2014, pp. 1676–1682.

[183] M. Budhia, J. T. Boys, G. A. Covic, and C.-Y. Huang, "Development of a single-sided flux magnetic coupler for electric vehicle IPT charging systems," *IEEE Trans. Ind. Electron.*, vol. 60, no. 1, pp. 318–328, Jan. 2013.

[184] A. Zaheer, D. Kacprzak, and G. A. Covic, "A bipolar receiver pad in a lumped IPT system for electric vehicle charging applications," in *Proc. IEEE Energy Convers. Congr. Expo. (ECCE)*, Sep. 2012, pp. 283–290.

[185] J. Wang, S. L. Ho, W. N. Fu, and M. Sun, "Analytical design study of a novel witricity charger with lateral and angular misalignments for efficient wireless energy transmission," *IEEE Trans. Magn.*, vol. 47, no. 10, pp. 2616–2619, Oct. 2011.

[186] J. I. Agbinya and N. F. A. Mohamed, "Design and study of multi-dimensional wireless power transfer transmission systems and architectures," *Int. J. Electr. Power Energy Syst.*, vol. 63, pp. 1047–1056, Dec. 2014.

[187] C. Park, S. Lee, G.-H. Cho, and C. T. Rim, "Innovative 5-m-off-distance inductive power transfer systems with optimally shaped dipole coils," *IEEE Trans. Power Electron.*, vol. 30, no. 2, pp. 817–827, Feb. 2015.

[188] M. Budhia, G. A. Covic, and J. T. Boys, "Design and optimization of circular magnetic structures for lumped inductive power transfer systems," *IEEE Trans. Power Electron.*, vol. 26, no. 11, pp. 3096–3108, Nov. 2011.

[189] S. Cheon, Y.-H. Kim, S.-Y. Kang, M. L. Lee, J.-M. Lee, and T. Zyung, "Circuit-model-based analysis of a wireless energy-transfer system via coupled magnetic resonances," *IEEE Trans. Ind. Electron.*, vol. 58, no. 7, pp. 2906–2914, Jul. 2011.
[190] D. Ahn, M. Kiani, and M. Ghovanloo, "Enhanced wireless power transmission using strong paramagnetic response," *IEEE Trans. Magn.*, vol. 50, no. 3, pp. 96–103, Mar. 2014.
[191] D. Ahn and S. Hong, "A transmitter or a receiver consisting of two strongly coupled resonators for enhanced resonant coupling in wireless power transfer," *IEEE Trans. Ind. Electron.*, vol. 61, no. 3, pp. 1193–1203, Mar. 2014.
[192] J. Kim, H.-C. Son, K.-H. Kim, and Y.-J. Park, "Efficiency analysis of magnetic resonance wireless power transfer with intermediate resonant coil," *IEEE Antennas Wireless Propag. Lett.*, vol. 10, pp. 389–392, 2011.
[193] R. Huang, B. Zhang, D. Qiu, and Y. Zhang, "Frequency splitting phenomena of magnetic resonant coupling wireless power transfer," *IEEE Trans. Magn.*, vol. 50, no. 11, pp. 1–4, Nov. 2014.
[194] E. Waffenschmidt, "Dynamic resonant matching method for a wireless power transmission receiver," *IEEE Trans. Power Electron.*, vol. 30, no. 11, pp. 6070–6077, Nov. 2015.
[195] D. Ahn and S. Hong, "Effect of coupling between multiple transmitters or multiple receivers on wireless power transfer," *IEEE Trans. Ind. Electron.*, vol. 60, no. 7, pp. 2602–2613, Jul. 2013.
[196] M. Fu, T. Zhang, X. Zhu, and C. Ma, "A 13.56 MHz wireless power transfer system without impedance matching networks," in *Proc. IEEE Wireless Power Transf. (WPT)*, May 2013, pp. 222–225.
[197] T. Duong and J.-W. Lee, "A dynamically adaptable impedance-matching system for midrange wireless power transfer with misalignment," *Energies*, vol. 8, no. 8, pp. 7593–7617, Jul. 2015.
[198] M. Fareq, M. Fitra, M. Irwanto, H. S. Syafruddin, N. Gomesh, Y. M. Irwan, M. A. Halim, A. Herman, and T. Hussain, "50 cm air gap wireless power transfer by magnetic resonance coupling," *Appl. Mech. Mater.*, vol. 785, pp. 205–209, Aug. 2015.
[199] R. Pinto, V. Lopresto, and A. Genovese, "Human exposure to wireless power transfer systems: A numerical dosimetric study," in *Proc. 11th Eur. Conf. Antennas Propag. (EUCAP)*, Mar. 2017, pp. 988–990.
[200] P.-P. Ding, L. Bernard, L. Pichon, and A. Razek, "Evaluation of electromagnetic fields in human body exposed to wireless inductive charging system," *IEEE Trans. Magn.*, vol. 50, no. 2, pp. 1037–1040, Feb. 2014.
[201] V. De Santis, L. Giaccone, and F. Freschi, "Influence of posture and coil position on the safety of a WPT system while recharging a compact EV," *Energies*, vol. 14, no. 21, p. 7248, Nov. 2021.
[202] V. Cirimele, F. Freschi, L. Giaccone, L. Pichon, and M. Repetto, "Human exposure assessment in dynamic inductive power transfer for automotive applications," *IEEE Trans. Magn.*, vol. 53, no. 6, pp. 1–4, Jun. 2017.
[203] A. El-Shahat, J. Danjuma, A. Y. Abdelaziz, and S. H. E. Abdel Aleem, "Human exposure influence analysis for wireless electric vehicle battery charging," *Clean Technol.*, vol. 4, no. 3, pp. 785–805, Aug. 2022.
[204] International Commission on Non-Ionizing Radiation Protection, "Gaps in knowledge relevant to the 'Guidelines for limiting exposure to time-varying electric and magnetic fields (1 Hz-100 kHz) Health physics,'" *Health physics,* , vol. 118, pp. 533–542, May 2020.
[205] International Commission on Non-Ionizing Radiation Protection, "ICNIRP Guidelines for limiting exposure to time-varying electric and magnetic fields (1 Hz to 100 kHz)," *Health Phys.*, vol. 99, no. 6, pp. 818–836, 2010.
[206] G. Ziegelberger, R. Croft, M. Feychting, A. C. Green, A. Hirata, and G. d'Inzeo, "Guidelines for limiting exposure to electromagnetic fields (100 kHz to 300 GHz)," Tech. Rep., 2020.
[207] International Commission on Non-Ionizing Radiation Protection, "Guidelines for limiting exposure to Electromagnetic Fields (100 kHz to 300 GHz)," *Health Phys.*, vol. 118, no. 5, pp. 483–524, May 2020.
[208] K. Miwa, T. Takenaka, and A. Hirata, "Electromagnetic dosimetry and compliance for wireless power transfer systems in vehicles," *IEEE Trans. Electromagn. Compat.*, vol. 61, no. 6, pp. 2024–2030, Dec. 2019.
[209] G. Battapothula, C. Yammani, and S. Maheswarapu, "Multi-objective optimal scheduling of electric vehicle batteries in battery swapping station," in *Proc. IEEE PES Innov. Smart Grid Technol. Eur. (ISGT-Eur.)*, Sep. 2019, pp. 1–5.
[210] R. Mehta, D. Srinivasan, and A. Trivedi, "Optimal charging scheduling of plug-in electric vehicles for maximizing penetration within a workplace car park," in *Proc. IEEE Congr. Evol. Comput. (CEC)*, Jul. 2016, pp. 3646–3653.
[211] M. L. Crow, "Electric vehicle scheduling considering co-optimized customer and system objectives," *IEEE Trans. Sustain. Energy*, vol. 9, no. 1, pp. 410–419, Jan. 2018.
[212] G. A. Covic and J. T. Boys, "Modern trends in inductive power transfer for transportation applications," *IEEE J. Emerg. Sel. Topics Power Electron.*, vol. 1, no. 1, pp. 28–41, Mar. 2013.
[213] Q. Wei, W. Guo, X. Sun, G. Wang, X. Zhao, F. Li, and Y. Li, "A new type of IPT system with large lateral tolerance and its circuit analysis," in *Proc. Int. Conf. Connected Vehicles Expo. (ICCVE)*, Dec. 2012, pp. 311–315.
[214] J.-U.-W. Hsu, A. P. Hu, and A. Swain, "A wireless power pickup based on directional tuning control of magnetic amplifier," *IEEE Trans. Ind. Electron.*, vol. 56, no. 7, pp. 2771–2781, Jul. 2009.
[215] N. Rathi, A. Ahmed, and R. Kumar, "Comparative study of soft switching and hard switching for brushless DC motor," *Int. J. Recent Trends Elect. Electron. Eng.*, vol. 1, pp. 1–5, May 2011.
[216] A. F. A. Aziz, M. F. Romlie, and Z. Baharudin, "Review of inductively coupled power transfer for electric vehicle charging," *IET Power Electron.*, vol. 12, no. 14, pp. 3611–3623, Nov. 2019.
[217] Z. Huang, S.-C. Wong, and C. K. Tse, "Design of a single-stage inductive-power-transfer converter for efficient EV battery charging," *IEEE Trans. Veh. Technol.*, vol. 66, no. 7, pp. 5808–5821, Jul. 2017.